Cent. Eur. For. J. 72 (2026) 3–26 Paradigm DOI: 10.2478/forj-2025-0018
CENTRAL EUROPEAN Forestry Journal

ORIGINAL PAPER

Assessing the influence of ground-based LiDAR devices, processing solutions, and forest stand characteristics on tree diameter and height estimation

Jozef Výbošťok[1]*, Juliána Chudá[1], Michal Skladan[1], Daniel Tomčík[1], Arunima Singh[2], Martin Mokroš[1, 3]

[1]*Technical University in Zvolen, Department of Forest Harvesting, Logistics and Ameliorations, T. G. Masaryka 24, SK-960 01 Zvolen, Slovakia*

[2]*Q-ForestLab, Ghent University, Department of Environment, Coupure Links 653, B-9000 Gent, Belgium*

[3]*University College London, Department of Geography, North-West Wing, Gower Street, UK-WC1E 6BT London, United Kingdom*

Abstract

Diameter at breast height (DBH) and tree height (TH) are essential parameters for accurately estimating tree volume, biomass, and other forest metrics. Conventional measurement methods often involve considerable time investment, which has motivated the development of approaches using 3D point cloud technology. These point clouds can be generated by terrestrial laser scanning (TLS), handheld mobile laser scanning (HMLS), or smartphone-based LiDAR. This study aims to determine which factor most significantly affects DBH and TH measurement accuracy. We evaluated multiple devices – specifically, TLS (FARO Focus S150), two HMLS devices (GeoSLAM ZEB Horizon and Stonex X120GO), and a smartphone (iPhone 13 PRO MAX), and processed their point clouds using two most perspective algorithms: FSCT and 3DFin. Data collection spanned forest plots differing in tree species composition and density: low- and high-density beech plots (*Fagus sylvatica* L.); high-density spruce plot (*Picea abies* [L.] H. Karst.); and high- and low-density mixed plots comprising *Abies alba* Mill., *Acer pseudoplatanus* L., *Fagus sylvatica* L., *Fraxinus excelsior* L., and *Picea abies* [L.] H. Karst. Across all devices and approaches used for DBH estimation, coefficient determination (R2) ranged from 0.692 to 0.998, RMSE from 1.24 to 6.73 cm, and relative RMSE from 4.30% to 42.7%, and bias from –1.84 to 3.50 cm. For TH estimation, R^2 ranged from 0.539 to 0.997, RMSE from 0.38 to 3.72 m, relative RMSE from 1.68% to 12.9%, and bias from –1.84 to 1.76 m. The results definitely showed that the accuracy of DBH estimation is significantly impacted by the device used and plot characteristics playing a secondary role, whereas TH accuracy depends largely on the selected algorithm. FSCT exhibited notably lower root mean square error (RMSE) for TH, with an average 1.6 m, compared to 2.4 m for the 3DFin. Across all test conditions, TLS consistently reached the smallest errors, while HMLS devices produced comparable results, and smartphone-based LiDAR demonstrated the highest variability.

Key words: terrestrial laser scanning (TLS); handheld mobile laser scanning (HMLS); 3D Forest Inventory (3DFIN); Forest Structural Complexity Tool (FSCT); iPhone-based scanning; forest inventory methods

Editor: Bohdan Konôpka

1. Introduction

Information about forest resources is essential for effective forest management. Diameter at breast height (DBH) is one of the most important directly measurable tree parameters in forest inventory. In contrast, tree height (TH) of standing trees often requires indirect estimation, although stem length can be measured directly on felled trees. These parameters are essential for calculating other important characteristics, including wood volume, biomass, and accumulated carbon (Wang et al. 2019; Balenović et al. 2021).

Accurate measurement of DBH is essential in forestry, but conventional tools such as diameter tape or caliper are labour-intensive, time-consuming, and limited over large areas (Cabo et al. 2018b; Chen et al. 2019; Mokroš et al. 2021). Calipers and diameter tapes are widely regarded as standard field instruments, pro-

*Corresponding author. Jozef Výbošťok, e-mail: xvybostokj@is.tuzvo.sk

viding high precision (e.g., standard deviation ~0.3 cm (Luoma et al. 2017)), yet their use becomes inefficient in dense stands or extensive inventories. Alternative manual approaches are simple and low-cost but less accurate and more sensitive to operator error (Binot et al. 1995). While DBH can be obtained with relatively high accuracy, assessing tree height is inherently more challenging. Measuring tree height is even more demanding, as it requires indirect determination of the distance between the tree base and top, typically by angle measurements, while stem length can only be directly obtained on felled trees.

Determining true TH requires identifying the crown top, which is difficult in broad-crowned deciduous trees but easier in conifers. Traditional methods include clinometers and hypsometers, which generally achieve sub-meter accuracy (Luoma et al. 2017; Martin 2022). However, geometric techniques such as the tangent or sine method can introduce bias: the tangent method is unbiased but variable, while the sine method systematically underestimates height by up to 20% (Larjavaara & Muller-Landau 2013). Simple stick or thumb rules are the least accurate, often with errors exceeding 10–15% (Saliu et al. 2021). Earlier measurements relied on direct methods, such as poles or destructive sampling, whereas indirect approaches using hypsometers, rangefinders, or total stations estimate height from angles and distances to visible points. Additionally, remote sensing techniques, such as aerial photogrammetry, Light Detection and Ranging (LiDAR), or Interferometric Synthetic Aperture Radar (InSAR), offer effective solutions for estimating TH without the need for direct or destructive methods (Krause et al. 2019). UAV-based photogrammetry has shown sub-meter accuracy in height retrieval, with reported RMSE below 0.8 m in mixed-species plots compared to ground measurements.

The rapid development of 3D modelling technologies has enabled the creation of highly detailed and accurate models using various laser scanners. Ground-based LiDAR devices are generally divided into terrestrial (TLS) and mobile systems (MLS) (Hyyppa et al. 2020). A separate category is represented by hybrid scanners, such as the RIEGL VZ-600i), FARO Orbis, or Stonex X200GO, which combine both stationary and mobile acquisition modes (VZ-600i Terrestrial Laser Scanning System, FARO Orbis Mobile Laser Scanner; STONEX X200GO SLAM Laser Scanner).

TLS produces the highest quality point clouds and the most accurate DBH estimations, but its use is limited by high costs, time demands, large datasets, and challenging terrain, making it more suitable for detailed monitoring of small areas (Liang et al. 2014; Liang et al. 2018; Kükenbrink et al. 2022).

Data collection typically relies on two approaches: single scans, which are fast but prone to occlusion and missed trees, and multi-scans, which are more time- and data-intensive but provide a more complete and accurate dataset (Astrup et al. 2014; Liang et al. 2016; Ritter et al. 2020).

Mobile Laser Scanners (MLS) reduce occlusion by capturing plots from multiple perspectives while in motion. They can be handheld (HMLS), worn in backpacks, or mounted on platforms, and rely on SLAM (Simultaneous Localization and Mapping) technology to estimate the device trajectory and register partial point clouds into a coherent 3D representation of the environment (Bauwens et al. 2016; Balenović et al. 2021; Mokroš et al. 2021). The major advantage of using MLS is the fast data collection over the entire research plot, with no need for equipment calibration or the logistical challenges associated with tripod-based setups or targets placement (Gollob et al. 2020). Compared to the TLS, the MLS device is lightweight and easy to carry, which allows easy movement through the forest (Balenović et al. 2021). However, compared to TLS, MLS provides lower spatial accuracy in point density and positioning, and its noisier point clouds may lead to false tree detections, particularly in dense forests (Mokroš et al. 2021).

Mobile devices with built-in LiDAR, such as iPads or iPhones, offer a low-cost alternative for point cloud acquisition, though their range is limited to about 5 m (Gollob et al. 2021; Mokroš et al. 2021). Applications like 3D Scanner or ForestScanner enable DBH measurements and spatial data collection directly in the field (Tatsumi et al. 2022). Although less accurate than TLS or MLS, these devices are more affordable and accessible, and in some cases can save time compared to traditional dendrometric methods, depending on accuracy requirements and area coverage (Gollob et al. 2021).

Research has therefore shifted to developing algorithms that derive tree metrics from remote sensing data for practical use. Among them, the Forest Structural Complexity Tool (FSCT) and 3DFin have been thoroughly tested, shown to be robust, and are ready for application. FSCT is a fully automated, sensor-agnostic open-source Python package capable of processing point clouds from TLS, MLS, UAV-LiDAR, or photogrammetry, though its command-line interface may limit accessibility (Krisanski et al. 2021). In contrast, 3DFin is a more user-friendly open-access tool available as a plugin in CloudCompare and QGIS or as a standalone program (Laino et al. 2024). Both tools analyse 3D point clouds to estimate forest structure and parameters such as DBH, TH, tree position, canopy cover, height variance, or volume.

The scientific community has taken different approaches to assessing measurement accuracy at the stand/tree level. Previous studies have evaluated various data sources and methodologies, including different types of TLS systems and scanning patterns (Liang et al. 2018; Kükenbrink et al. 2022), MLS approaches (Ryding et al. 2015; Cabo et al. 2018a; Tupinambá-Simões et al. 2023), and in-house developed devices (Hyyppä et al. 2020) while also reporting tree detection rates based on

plot characteristics and the growing season during which the data were collected (Liang et al. 2018; Kükenbrink et al. 2022; Tupinambá-Simões et al. 2023).

In recent years, the scientific community has increasingly focused on developing systems for automated forest inventory, from hybrid SLAM solutions such as HCTO (Li et al. 2024) (Optimality-Aware LiDAR Inertial Odometry) or multi-sensor compact helmet-based scanners for real-time measurement of dendrometric parameters in the field (Li et al. 2023). Before advanced technologies can be adopted in routine practice, it is necessary to address fundamental questions of reliability, accuracy, and usability of currently available devices, considering both researchers and forest managers.

Previous studies have provided numerical benchmarks for the expected accuracy of ground-based laser scanning methods. In a large international benchmarking, Liang et al. (2018) reported DBH RMSE values commonly between 1 and 4 cm, with conservative algorithms achieving 1–3 cm and robust algorithms 2–4 cm across different forest conditions. For tree height, TLS typically reached errors within 0.5–1.0 m, though canopy occlusion occasionally increased uncertainty. Similarly, Kükenbrink et al. (2022) found that HMLS devices can achieve DBH accuracy close to TLS, with mean deviations below 2–3 cm, while tree height errors generally remained under 1 m in open stands but increased in denser canopies.

Despite the emphasis on innovative technologies, a fundamental question still lingers – what are the key factors that influence the estimation of DBH and TH?

Although numerous studies have reported DBH measurements using TLS, relatively few have investigated the factors influencing the accuracy and determination of DBH (Bauwens et al. 2016; Cabo et al. 2018a; Liu et al. 2018; Kükenbrink et al. 2022; Guenther et al. 2024). Despite the separate articles devoted to each topic, there is no comprehensive article that addresses all the issues. Therefore, the main objective of this study is to find out which factor influences the determination of DBH and TH measurement accuracy the most, whether it is device, algorithm, or the characteristics of the forest plot.

Regarding TH, the same authors have reported several findings that reflect the current state of the art in this area: Liu et al. (Liu et al. 2018) investigates methods for using TLS to obtain point cloud cover and estimating TH and DBH at plot level in areas of difficult terrain. Kükenbrink et al. (Kükenbrink et al. 2022) points out the limitations of the range of the HMLS device, which with a maximum range of 30 m, is not able to acquire top of the canopy. Consistently, Bauwens et al. (2016) notes that current equipment does not always allow scanning of the top of the canopy layer, which is crucial for accurate timber and biomass volume estimates. Cabo et al. (2018a) compares the use of wearable laser systems (WLS) – backpack or handheld, and terrestrial laser scanners (TLS) to automatically detect trees and estimate their DBH and TH. Guenther et al. (Guenther et al. 2024) reviews recent and cost-effective low-range technologies that are promising for forestry but do not yet allow TH to be inferred due to limited range.

Our study focuses on investigating factors that may influence the accuracy of the estimation of the two most important tree parameters. This is a key issue for forestry, and our study aims to provide a comprehensive view of ground-based remote sensing technologies, specifically focusing on how well these methods extract forest parameters such as DBH and TH.

This study compares TLS (FARO Focus 3D S150), MLS devices (Stonex X120GO SLAM and GeoSLAM ZEB Horizon) and an iPhone 13 PRO MAX which is equipped with a LiDAR sensor, on plots characterized by different tree species composition and density. The two most recent and promising algorithms, namely FSCT and 3DFin, were used to determine DBH and tree TH.

In this study, we aim to conduct a comprehensive comparison of these devices under varying conditions in Central European forests, using different algorithms, to develop a clear and efficient methodology for forest data collection. To the best of our knowledge, no comprehensive study has yet addressed this key question, leaving both researchers and practitioners without a complete understanding of this essential aspect of forest ecosystem analysis.

2. Materials and methods

2.1. Test plots

The study sites are situated within the University Forest Enterprise of the Technical University in Zvolen, positioned at the centre of Slovakia, in the Kremnica mountains (Fig. 1).

Five distinct research forest plots, each measuring 30 × 30 meters, were carefully chosen to encompass varied species, age distributions, and densities. The investigation encompassed a total of 396 individual trees. These plots were specifically categorized as follows: low-density, mature European beech forest (*Fagus sylvatica* L.) (beech old – BO); high-density, young European beech forest (*Fagus sylvatica* L.) (beech young – BY); high-density, young Norway spruce forest (*Picea abies* [L.] H. Karst.) (spruce young – SY); high-density, young mixed forest (mixture young – MY); and low-density, mature mixed forest (mixture old – MO). Composition of mixed forests is mostly Silver fir (*Abies alba* Mill.), Sycamore maple (*Acer pseudoplatanus* L.), European beech, European Asch (*Fraxinus excelsior* L.) and Norway spruce. The mean DBH of all trees were 20.01 cm. The largest average diameter was 28.9 cm in the mixture old plot, while the smallest average diameter was 16.17 cm at the Beech young plot (Fig. 2).

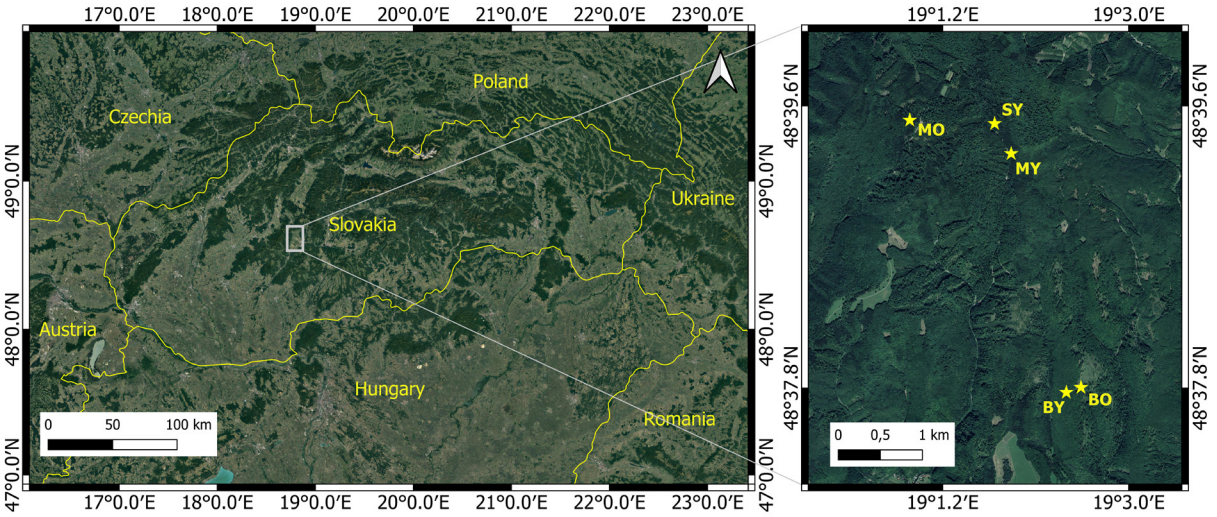

Fig. 1. Position of the research plots within Slovakia. MO – mixture old, MY – mixture young, SY – spruce young, BY – beech young, BO – beach old. (Sources: Satellite imagery © Google, Maxar Technologies 2024; Orthophoto mosaic © Geodetic and Cartographic Institute Bratislava, National Forest Centre 2022).

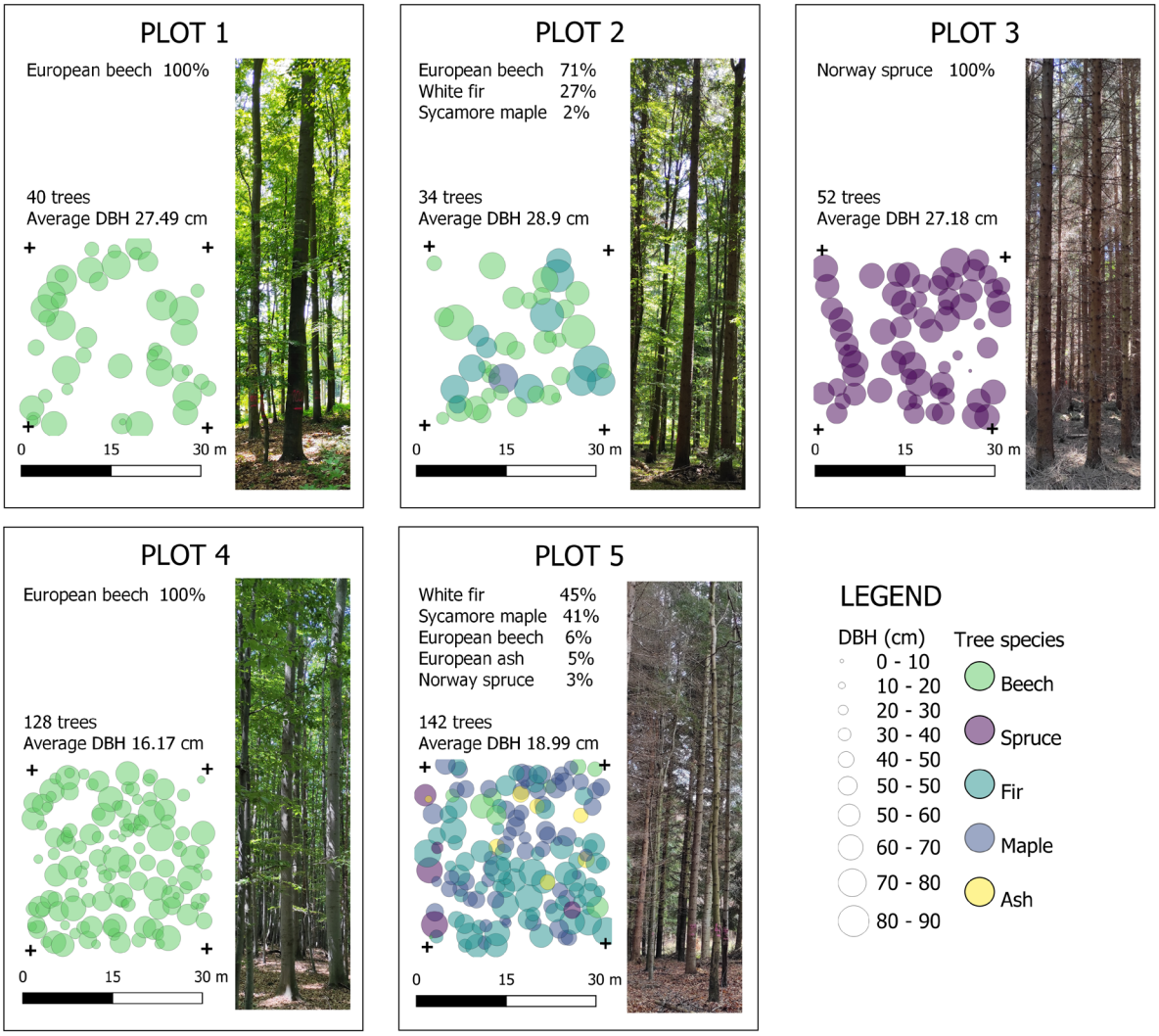

Fig. 2. Diameter at the Breast Height, species, density and number of trees within research plots.

2.2. Reference data collection

Firstly, each test plot with dimensions 30 × 30 m was stabilized in field. It implies, the corners of the plots were permanently fixed with ground control points (GCP) – (survey anchors) and measured using a Stonex GNSS receiver combined with a Topcon 9000 GNSS total station, subsequently these points enabled georeferencing and enhance spatial orientation during data collection. The anchors positions were measured using standard geodetic methods, achieving a positional accuracy of less than 2 cm. After establishong the plots, all tree positions were measure by a total station. All data were collected from one total station position in the middle of the plots, and two corner points were used as orientation points. The position for the total station was chosen so that all trees could be seen from one place (it was possible in most cases). During the position measurements, individual trees were numbered with spray paint, and their species were identified. DBH was measured by diameter tape at 1.3 m height, always from the uphill side of the tree. Tree positions were defined as the center of the stem at breast height (DBH). In the field, a single point was measured on the stem surface using a total station. During post-processing, the measured distance was corrected by subtracting the stem radius along the measured azimuth, ensuring that the resulting coordinates represented the stem center. In cases where trees were not directly visible due to occlusion, additional total station setups were established to acquire the necessary measurements.These meticulously recorded data served as a reference for comparing the parameters obtained from the point clouds collected using selected methods.

For reference TH values, manual measurements were derived from TLS point clouds. No traditional field measurements of tree height were performed, as TLS provides highly accurate and objective data, enabling complete coverage of all trees within the plots (Calders et al. 2015; Liang et al. 2016; Wilkes et al. 2017; Rouzbeh Kargar et al. 2020; Li et al. 2023). Although this approach relies on TLS data, it is not intended as a standard procedure due to its time-consuming nature; rather, it serves as a valid benchmark, as described in the next section. To extract reference TH, individual trees were manually segmented in the open-source software CloudCompare v2.12beta (http://cloudcompare.org/). After selection, the height of each tree was measured using the Point Picking tool as the distance between two points, from the ground level at the uphill side of the stem base (h = 0) to the tree top (Wardius & Hein 2024). We ensured that during height measurement the endpoint is always defined as the highest point within the crown of the specific tree. This means that if a lateral branch is the highest point, it is deliberately considered as the tree height.

2.3. Terrestrial laser scanning

In the experiment, we used a FARO Focus S150 laser scanner for data collection using the multi-scan method. Before starting the scanning process, reference spheres were placed within the research plot. During each scan, 12 spheres were evenly distributed, 8 spheres were positioned outside the plot's boundary (2 on each side), and an additional 4 spheres were placed within the plot area. The arrangement of the spheres and the scanner followed the configuration depicted in Fig. 3a. With careful adjustment, each position was optimized to maximize visibility of the spheres from multiple scanner angles. Each research plot was scanned from 13 distinct positions, with 5 positions located within the plot and 8 positions situated around its boundary. The scanning procedure was initiated from the centre of the research plot, scanning both the interior and the surrounding borders. The duration of a single scan was approximately 4 minutes and 25 seconds. And the entire scanning operation, inclusive of sphere placement, scanner positioning, and stabilization, took approximately 2 hours and 20 minutes to 2 hours and 40 minutes, contingent upon the ruggedness of the terrain and the density of vegetation. At each scanner position, we ensured optimal visibility of as many spheres as possible, with a minimum of four spheres positioned nearby. Furthermore, it was imperative to ensure that the reference spheres remained undisturbed throughout the entirety scanning process.

2.4. Mobile laser scanning

In this experiment, we implemented two HMLS devices, Stonex X120GO SLAM and GeoSLAM ZEB Horizon. These devices had very similar technical specifications (Table 1). The most significant difference was that when using the MLS Stonex X120GO, in addition to the scanner itself, it was necessary to use a mobile Android device with an application from the manufacturer, GOapp, which allowed us to monitor the scan progress in real time and record GCPs, as well as to initialize, start, and stop the scan. In addition, the scanner from Stonex is equipped with three 5 Megapixels cameras, enabling the production of colour point clouds. Generating colour point clouds with the GeoSLAM scanner requires purchasing the ZEB Vision add-on, whereas the Stonex X120GO SLAM provides colour point clouds natively, without any extra hardware or software. Another significant difference between the two devices is their purchase price, which is almost twice the price of the Stonex device. The Stonex X120GO can be purchased almost €15 000 cheaper than a device with similar parameters GeoSLAM Zeb Horizon (approx. Stonex €35 000, GeoSLAM €50 000). The method of data collection for HMLSs devices was identical. The operator scanned with the HMLS device carried in their hands,

starting at the corner of the research plot, and proceeding parallel to the edge of the plot; the area was scanned in strips with 10 meters of spacing. The georeferencing of plots were also done by recording the GCP with known position to know the local coordinate system (in our case S-JTSK). The scanning procedure is shown in Fig. 3. We planned the HMLS data collection according to our previous research. Entire scanning procedure lasted approximately 4 minutes for each of the systems (Chudá et al. 2024; Skladan et al. 2025).

2.5. Data processing

The last device we evaluated in this study is the iPhone 13 PRO MAX, which is equipped with an Apple LiDAR sensor. We have used a 3D Scanner app application that generates point clouds in real-time. Compared to other 3D-scanning solutions the 3D Scanner App stands out because its cost-effectiveness, simplicity and rapid point-cloud capture and subsequent dendrometric analysis (3D Scanner App).

The scanning scheme was done in a way to cover each tree in the plots by going around the trees starting from the corner of the plots. The scanning trajectory was adjusted to the maximum range of the iPhone LiDAR scanner, which is 5 meters. The detailed description of the scanning trajectory is depicted in the (Fig. 3c). It is important to observe the proximity of the trees; we considered two trees as one if they were found to be very close to each other. Total estimated time recorded for data collection using iPhone was approximately 5 minutes. A detailed comparison of specification is shown in (Table 1).

2.6. Data processing

The pre-processing and generation of point cloud was done using the device-specific software. GeoSLAM HUB was used to generate point clouds from GeoSLAM while GOpost was employed for the Stonex system. FARO Scene software to process point cloud from FARO Focus which not only allowed us to generate a point cloud but also to merge all the scans, based on their positions within the plot, into a single final scan. The integration of the point clouds into the final scan was achieved using reference spheres and targets strategically positioned within and around the plot. To refine the point clouds according to the GCP, LASclip function was used in LAStools (https://rapidlasso.de) program to clip the plots.

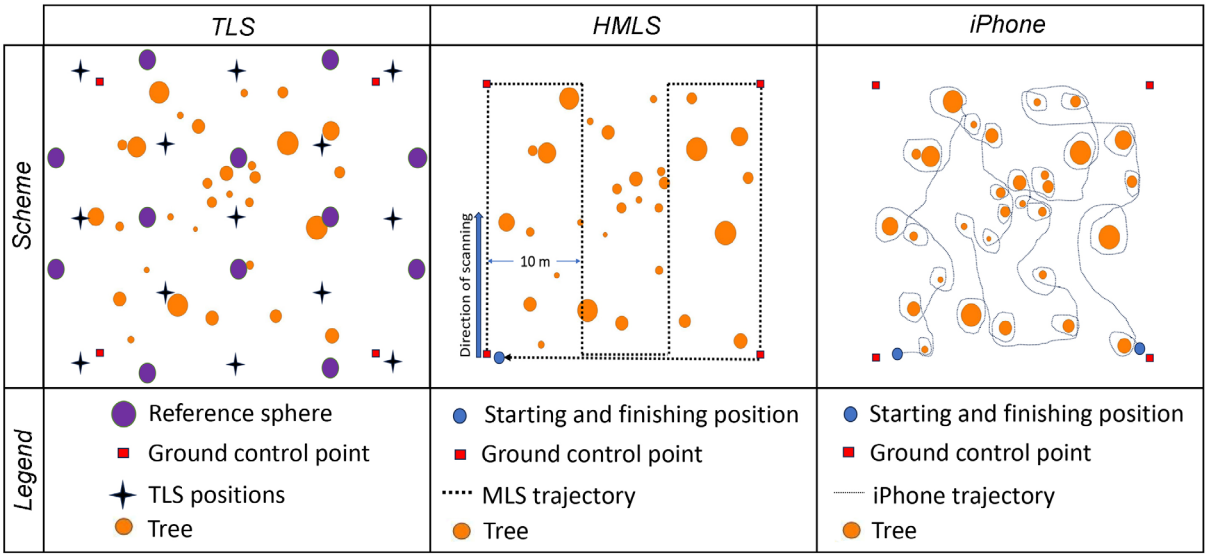

Fig. 3. Data acquisition by each method (A) shows the TLS location positions and the distribution of reference spheres within the research plot, (B) shows the scan trajectory using both HMLS, and (C) shows the scan trajectory using iPhone.

Table 1. Comparison of selected parameters of used technologies.

	Faro Focus S150[1]	GeoSLAM ZEB Horizon[2]	Stonex X120GO[3]	iPhone 13 Pro Max[4]
Measurement distance range (m)	0.6 – 150	100	0.5 – 120	Max. 5
Relative accuracy (mm)*	1	6	6	–
Scanning point frequency (pts/s)**	2 000 000	300 000	320 000	–
Weight (kg)	4.2	1.45	1.6	0.24
Acquisition time per plot (min)	140	4	4	5
Total points per plot (approx.)	70,000,000	27,000,000	24,000,000	9,000,000

Notes: [1]FARO – Terrestrial Scanner Focus S150 / S350 Plus, n.d.; [2]ZEB Horizon: The Ultimate Mobile Mapping Solution, n.d.,[3]X120GO SLAM Laser Scanner – Stonex, n.d.,[4]"iPhone 13 Pro a iPhone 13 Pro Max", n.d., *referring to the internal precision between points within the dataset, as specified by the manufacturer, ** the number of points measured per second.

2.7. Diameter at the Breast Height and Tree Height estimation

We used two different algorithms to determine the DBH (nominally 1.3 m above the ground) and TH (measured as the vertical distance from ground level to the highest point of the tree) of the trees. FSCT and 3DFin are used because they combine open-source accessibility, systematic validation, and broad adoption across the research. FSCT is an open-source Python tool developed for automated extraction of tree parameters from point clouds (Krisanski et al. 2021). It was implemented using Anaconda Navigator 2.4.0 ("Files : Anaconda.org" n.d.). The software provides DBH, TH, and tree volume estimates. DBH is calculated as the average diameter of cylinder segments between 1.0 and 1.6 m above the digital terrain model (DTM), while TH is derived by combining trunk cylinder segments with vegetation points and selecting the highest point. During stem segmentation, parameter values were adjusted to accommodate complex forest point clouds. Horizontal slicing was set to 0.15 m to balance capturing stem geometry with noise reduction, and a fine vertical shift of 0.05 m improved cylinder continuity at the cost of higher computational load. Stem sorting ensured consistent assignment of segments to individual trees. Tree height was derived from the maximum vegetation point (percentile = 100), with a 5 m minimum stem detection threshold applied to avoid misclassifying branches or deadwood. Taper analysis measured stem diameters up to 30 m height at 0.2 m intervals, using ±0.2 m slices; the largest fitted cylinder was retained to minimize noise and irregularities. This approach provides a robust taper curve, particularly in stands with well-defined central stems (Krisanski et al. 2021).

3DFin is a graphical tool implemented as a plugin in CloudCompare for tree detection and parameter estima-

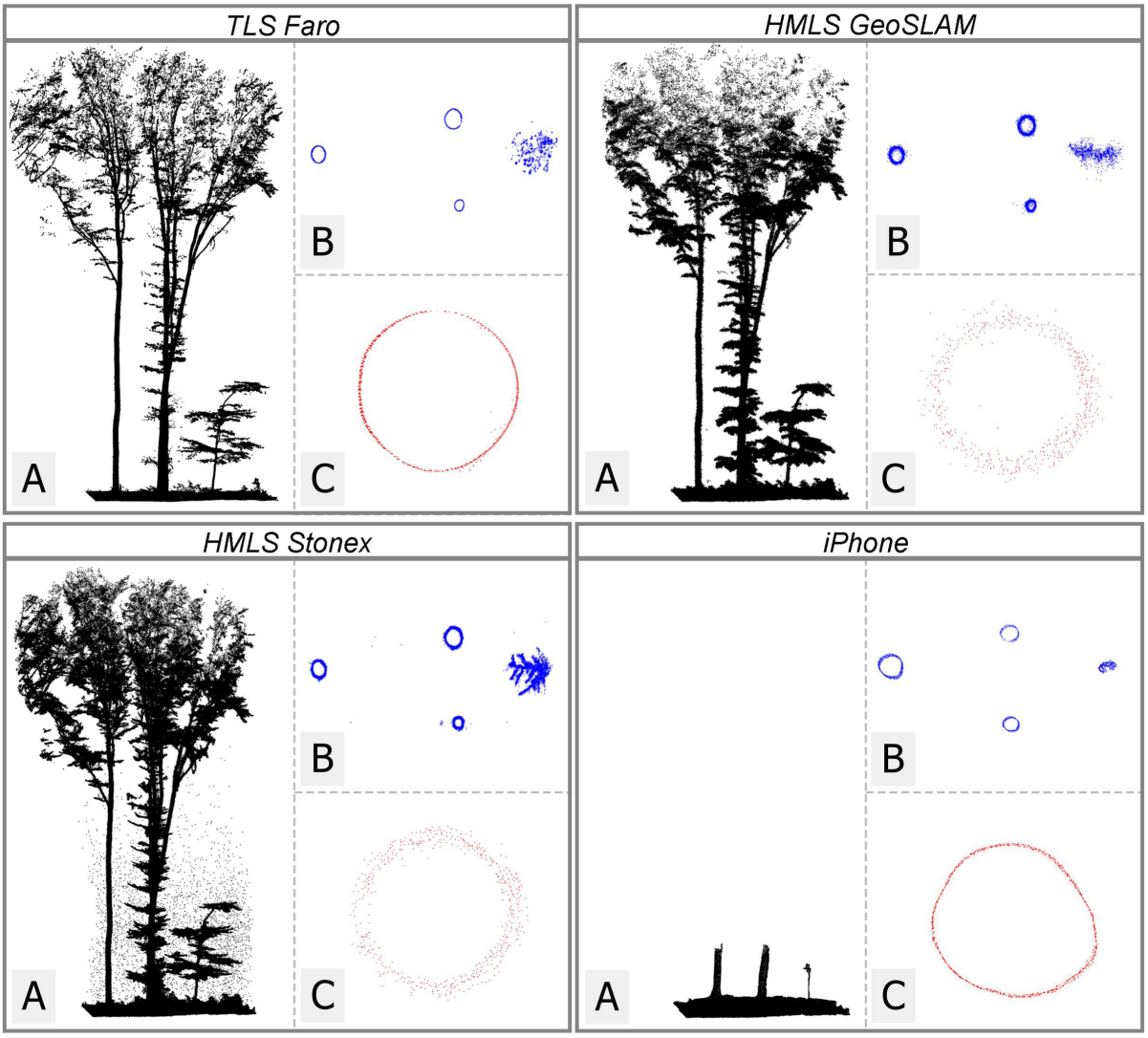

Fig. 4. Examples of the point clouds from all devices in the side view (black), 3 cm trunk cross-sections at 1.3 m height above the ground (blue), and tree cross-section detail (red).

tion from ground-based point clouds. It computes DBH using circle fitting through least-squares minimization, while TH is estimated from normalized point clouds by selecting the highest voxel within a defined radius around the tree axis (Laino et al. 2024). The configuration used for stem detection and measurement in 3DFin was point clouds acquired in structurally complex forest stands. The point cloud was normalized to the ground surface prior to segmentation, ensuring that height-based filtering and sectioning would operate on vertically consistent data. The algorithm focused on the height stripe between 0.7 m and 3.5 m above ground, which is typically where the stem is least occluded and vertically consistent. A moderate pruning intensity of 2 (scale 0–5) was applied to reduce noise and non-stem points within the stripe. The cloth resolution for DTM generation was set to 0.2 m, balancing terrain detail with smoothing over fine-scale surface variation.

To guide stem detection, the algorithm was configured with a minimum expected diameter of 0.09 m and a maximum expected diameter of 1.0 m. A stem search diameter of 2.0 m was applied to determine the neighbourhood extent considered during cylinder fitting. Circular sections were fitted from 0.3 m to 30.0 m above the ground, with a vertical spacing of 0.2 m between sections and a slice thickness of 0.05 m. These values allow a fine-grained taper profile to be computed, while remaining computationally efficient. A minimum of 80 points was required per section for reliable diameter estimation, and quality control criteria ensured at least 9 of 16 angular sectors within the circular slice were populated. The DBH was estimated by fitting circles to sections located within the stripe zone, using 200 points per circle and a drawing interval of 0.01 m. The algorithm placed the stem axis by evaluating vertical consistency across voxels sized 0.035 m × 0.035 m and associating points based on proximity to this axis within a 15 m search range. Tree height was computed using a voxel-based approach with a vertical resolution of 0.3 m, considering points associated with each individual stem. A maximum vertical deviation of 25° from the main axis was allowed to accommodate leaning trees. The final height metric corresponds to the topmost point assigned to the stem instance, provided that axis continuity and diameter constraints were met.

2.8. Data evaluation and statistics

Estimated DBH and TH values from the FSCT and 3DFin tools were compared with field data obtained using a diameter tape. The pairing was performed manually in QGIS for Desktop (QGIS Development Team, 2024, QGIS Geographic Information System, Version 3.16 [Software], Open-Source Geospatial Foundation, QGIS Web Site). Once all pairs were identified, estimation errors (EST_{err}) were calculated by subtracting the estimated values (V_{est}) from the reference measurements (V_{ref}) (equation 1).

$$EST_{err} = V_{est} - V_{ref} \quad [1]$$

where EST_{err} is a calculated error of estimated values, V_{est} is estimated value from point cloud via FSCT and 3DFin, V_{ref} is measured value in the field.

Data processing, organization, and statistical analyses were conducted using RStudio (Version 2023.12.1 Build 402). To evaluate the accuracy of DBH and TH estimation from LiDAR-based methods, we employed a multi-step statistical analysis approach. First, we calculated root mean square error (RMSE) (equation 2) and the coefficient of determination (R^2) (equation 3) to quantify the correlation and deviation between estimated and measured DBH and TH values across different devices, algorithms, and plots. These descriptive statistics provided an initial overview of estimation performance.

$$RMSE = \sqrt{\frac{\sum_{i=1}^{n} (y_i - \hat{y}_i)^2}{n}} \quad [2]$$

$$R^2 = \sqrt{\frac{\sum_{i=1}^{n} (y_i - \hat{y}_i)^2}{\sum_{i=1}^{n} (y_i - \bar{y}_i)^2}} \quad [3]$$

where y_i represent measured value, $\hat{y}_i$ represent estimated value, $\bar{y}$ is the average of the observed values and n is number of trees in dataset.

To assess whether differences between estimated and reference DBH and TH values were statistically significant, we used paired t-tests for each device, plot and algorithm combination. This allowed identification of over- or underestimation trends in specific forest conditions. A three-way ANOVA was then conducted to examine the effects of Device, Plot, and Algorithm on DBH and TH estimation error. Post-hoc comparisons were performed using Tukey's HSD test to identify statistically significant differences between specific device combinations. To further explore interaction effects between Plot, Device, and Algorithm, we computed Estimated Marginal Means (EMMs) based on a full-factorial ANOVA model. The EMMs were derived using the emmeans package in R to obtain adjusted mean error values for each combination of factors (i.e. Plot × Device × Algorithm). This approach allowed us to interpret group means while accounting for the influence of other factors in the model. This EMM based analysis complements the ANOVA by providing clear, interpretable comparisons of adjusted error values, especially useful for identifying device-specific performance differences across stand types and algorithmic approaches. To evaluate whether estimation accuracy is influenced by the size of DBH, we analyzed the relationship between measurement error and reference DBH using linear regression. To account for potential differ-

ences among measurement devices, we extended the model by including Device as a fixed effect and tested for interactions between reference DBH and Device. This allowed us to determine whether the slope of the error–DBH relationship differed among devices, i.e. whether some devices showed stronger size-related biases than others. Model assumptions were checked using residual diagnostics, and model fit was evaluated using R^2.

3. Results

3.1. Diameter at the breast height

Across all plots, there is a strong linear relationship between estimated and reference DBHs (see Appendix A1). The TLS achieved the highest correlation between measured and estimated data across all plots and methods. In general, the lowest corelation was achieved by the iPhone LiDAR. The highest correlation was obtained for TLS in old beech plots by the 3DFin algorithm ($R^2 = 0.992$) accompanied by a low residual standard error (RSE) 1.4 cm, and a relative RSE of only 5.1%. 3DFin – TLS combinations generally underestimated DBH values slightly, as reflected in negative mean residuals (e.g., –0.8 cm in old beech plot and –0.2 cm in mixture young plot) (Appendix A2).

On the contrary, the lowest correlation is observed for the iPhone LiDAR in young beech stands and data processed by the 3DFin algorithm ($R^2 = 0.692$) with a substantially higher RSE of 5.6 cm (35.6% relative RSE). Both, HMLS GeoSLAM, and Stonex achieved very similar correlation values.

The results indicate that the largest errors occur in areas covered by small trees, particularly in young stands (BY, SY, MY) which are significantly overestimated, especially by the iPhone (e.g., bias 3.5 cm in young beech plot).

In terms of correlation, the 3DFin algorithm generally achieved higher coefficient of determination ($R^2 = 0.948$) compared to FSCT ($R^2 = 0.929$). Regarding DBH RMSE, TLS consistently provided the lowest errors, while iPhone-based estimates consistently showed the highest errors (see Fig. 5). More specifically, TLS achieved the highest RMSE of 1.2 cm in the old beech plot, whereas iPhone reached peak RMSE of 6.7 cm in the DBH dataset estimated from the young beech plot. HMLS consistently demonstrated significant errors throughout the experiment. The largest errors, influenced by plot characteristics, occurred in young stands with thinner trees. Overall, the highest DBH RMSE occurred in the data gained in young spruce, while the lowest DBH RMSE was observed in old beech plots. Regarding the impact of the algorithm on DBH RMSE, the 3DFin performed better with an average error of 2.6 cm compared to 2.8 cm for FSCT.

The TLS point cloud processed with 3DFin showed no statistically significant difference between measured and estimated DBHs in any research plot. In contrast, the FSCT algorithm resulted in a statistically significant underestimation of DBH in the SY and MY plots. Both HMLS devices achieved similar RMSE values, with Stonex slightly overestimating DBH and GeoSLAM underestimating it. The iPhone exhibited the highest RMSE, with statistically significant differences between measured and estimated DBHs across all plots, except for the MO forest.

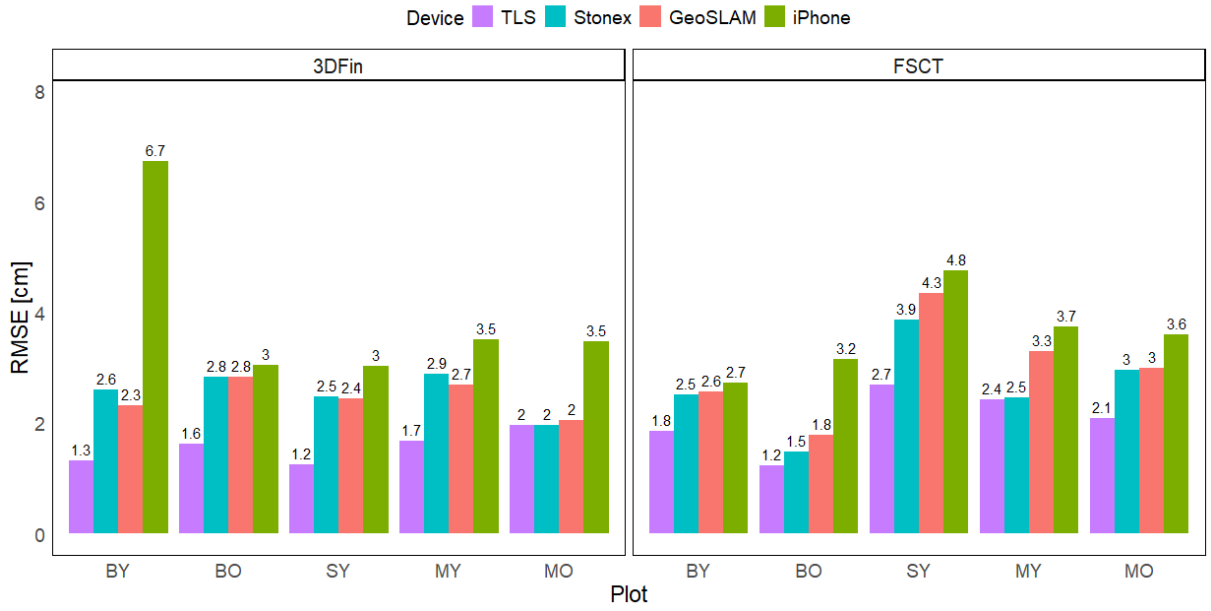

Fig. 5. Root mean square error for diameter at breast height. Bar plots show RMSE: Upper 3DFin based, lower FSCT based (BY – beech young, BO – beech old, SY – spruce young, MY – mixture young, MO – mixture old).

ANOVA results indicate that the device used for data collection has the greatest influence on DBH estimation (see Table 2). Although the plot also has a significant effect, its influence is lower than that of the device, and the algorithm does not have a statistically significant impact on the final DBH estimation.

Tukey's HSD test, performed as a post-hoc analysis following a 3-factor ANOVA (with factors Plot, Device, and Algorithm), revealed statistically significant differences in mean error values between devices. Specifically, the iPhone versus GeoSLAM comparison showed a mean difference of 2.9 cm (p-value = <0.0001), indicating that the iPhone produces significantly larger errors than GeoSLAM. The Stonex versus GeoSLAM comparison yielded a mean difference of 2.0 cm (p-value = <0.0001), with Stonex showing higher errors, while the TLS versus GeoSLAM comparison resulted in a mean difference of 0.5 cm (p-value = <0.001), indicating a statistically significant but smaller difference. Overall, TLS is clearly the most reliable device for both algorithms, and the iPhone shows the highest error rate, particularly in more complex stands (BY, SY, MO). GeoSLAM and Stonex represent suitable compromises that, while not always achieving the accuracy of TLS, offer significant time savings.

The analysis of estimated marginal means (Fig. 6) reveals statistically significant differences in diameter at breast height (DBH) estimates across the device types, depending on site and algorithm used. For TLS, errors were generally close to zero across most forest types, indicating no statistically significant bias when using the 3DFin algorithm. However, statistically significant differences ($p < 0.05$ or lower) were observed for the SY and MY forest types when using the FSCT algorithm. In contrast, DBH estimation using the iPhone (3DFin algorithm) resulted in the largest overestimations, particularly for BY (+3.26 cm) and MY (+2.18 cm), suggesting a systematic tendency toward overestimation with this device. Conversely, GeoSLAM (3DFin and FSCT algorithms) exhibited a consistent pattern of underestimation, with the most pronounced negative errors observed for MO (–1.84 cm) and SY (–1.73 cm). The magnitude of DBH measurement errors varied across different tree stands, with the SY and MO forest types exhibiting the largest deviations across most device and algorithm combinations. In contrast, BO and MY forest types displayed smaller errors across multiple measurement algorithms, indicating that these stands provided more favourable conditions for accurate DBH estimation.

The error distribution analysis (Appendix A3) highlights the fact that the accuracy of the DBH estimation is affected not only by the software used, but also by the specific equipment and stand structure. FSCT appears more stable overall, with fewer outliers, while 3DFin shows more variance, especially for the iPhone. TLS has mostly

Table 2. Analysis of variance results for diameter at breast height. The table presents degrees of freedom (Df), sum of squares (Sum Sq), mean square (Mean Sq), F-value, and associated p-value for the tested effects.

DBH	Df	Sum Sq	Mean Sq	F value	p-value
Device	3	4,036	1,245.2	177.579	<2e-16 ***
Plot	4	164	40.9	5.404	0.000247 ***
Algorithm	1	5	5.0	0.656	0.417875
Residuals	3,013	22,825	7.6		
Significant Codes	0	0.001 '***'	0.01 '**'	0.05 '*'	0.1 '.'

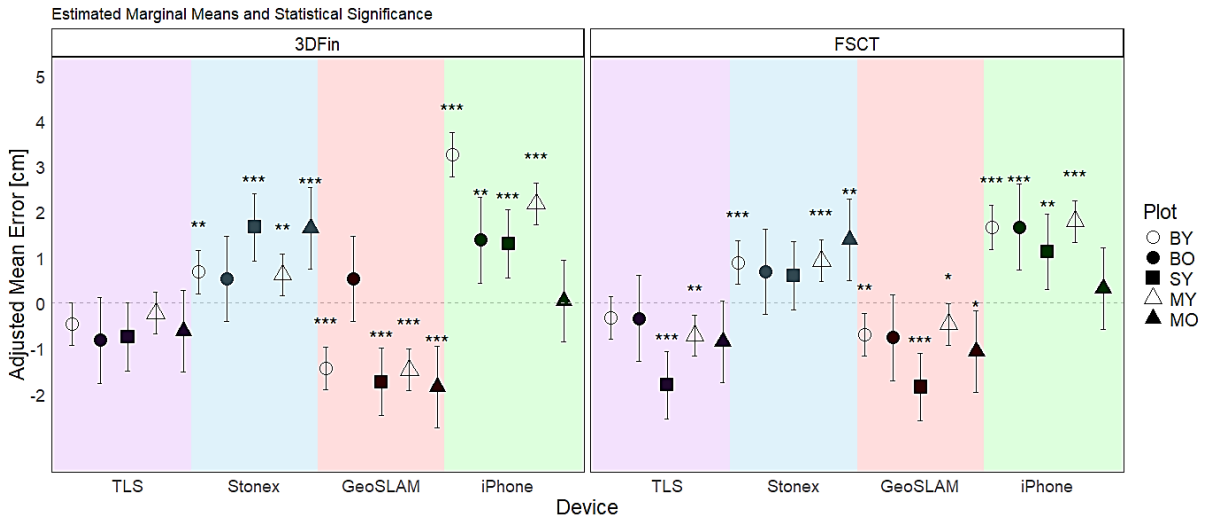

Fig. 6. Estimated Marginal Means of diameter at breast height according to each device used, and different sites and algorithm. Significant differences between estimated and reference DBH, according to each device used, different sites and algorithm, are indicated as follows: 0.001 '***', 0.01 '**', 0.05 '*'.

smaller error variance, but sometimes larger extremes appear. Stonex and GeoSLAM perform equal, whereas iPhone showing the largest fluctuations. The effect of age is especially evident in the younger stands (BY, SY, MY), where, on average, exhibit slightly higher mean errors across devices and approaches. However, the older stands (BO, MO) tend to show more pronounced differences in specific cases (e.g., BO – GeoSLAM, 3Dfin; MO – iPhone, 3DFin/FSCT).

To evaluate whether estimation accuracy was influenced by tree size, we analyzed the relationship between measurement errors and reference DBH (see Table 3). The analysis revealed that estimation error was influenced by tree size. Across all devices, error decreased with increasing DBH ($\beta = -0.060$, $p < 0.001$), indicating that smaller stems tended to be overestimated, whereas larger stems were measured more accurately. However, the error–DBH relationship varied among devices. For the iPhone, errors declined more sharply with increasing DBH ($\beta = -0.026$, $p = 0.015$), suggesting a stronger overestimation bias in smaller stems. The Stonex device showed a positive bias, but its size-related trend was no significant ($p = 0.821$). In contrast, TLS measurements did not show a significant overall bias ($p = 0.582$), but the interaction term was positive ($\beta = 0.031$, $p = 0.004$), resulting in a shallower negative slope (–0.029). This indicates that TLS performed well for smaller stems but tended to slightly underestimate larger stems. Overall, the extended model explained 22% of the variance in estimation error ($R^2 = 0.219$), a marked improvement over the model with DBH alone ($R^2 = 0.062$).

3.2. Tree height

For TH assessment, SY trees show the lowest RMSE, indicating the highest accuracy of TH measurements. The lowest RMSE was achieved with TLS (1.73 m), followed by GeoSLAM (2.00 m) and Stonex (2.21 m) and iPhone LiDAR was not viable. Trees in YM plot show a medium level of TH accuracy. Trees in OM stands reached similar RMSE across the devices. They are most accurate for TLS (2.49 m), while GeoSLAM (2.84 m) and Stonex (3.11 m) are slightly worse. Old beech stands reached the highest RMSE in all categories, especially when Stonex with 3DFin software (6.38 m) is used. The TH accuracy improves when using GeoSLAM (5.67 m) and is best with TLS (4.89 m). When BY plot is considering, RMSE is lower compared to BO plot. The best accuracy is achieved with TLS (3.57 m), while Stonex (4.44 m) and GeoSLAM (3.79 m) are slightly less accurate.

We conclude that, from an algorithmic perspective, 3DFin exhibits higher errors than FSCT (Fig. 7). HMLSs devices produce approximately the same errors, while TLS achieves the smallest error in all cases. FSCT generally achieves lower TH RMSE values, thus achieving more accurate results compared to 3DFin. For instance, in the young stand MY, FSCT achieved lower RMSEs compared to 3DFin: 1.19 m vs. 2.22 m (GeoSLAM), 1.34 m vs. 2.18 m (Stonex), and 0.54 m vs. 1.23 m (TLS). Similarly, in the mature stand MO, FSCT also resulted in substantially reduced RMSEs: 1.35 m vs. 2.14 m (GeoSLAM), 1.40 m vs. 2.47 m (Stonex), and 1.03 m vs. 1.50 m (TLS).The Fig. 7 confirms that the choice of algorithm (3DFin vs. FSCT) can significantly affect the resulting measurement error, with FSCT more often achieving lower TH RMSE values. There is no clear best system in terms of equipment; accuracy depends on the nature of the stand and the specific algorithm. When grouped by stand age, younger stands (BY, SY, MY) exhibited slightly lower mean errors compared to older stands (BO, MO). The average TH RMSE across all devices and algorithms for young stands was 1.57 m, while older stands averaged 2.14 m.

Tukey's HSD test was used as a post-hoc analysis after performing a 3-factor ANOVA (with the factors Plot, Device and Algorithm). For TH there are significant differences between spruce and beech. Other tree species comparisons are not statistically significant. There were no significant differences in mean errors between Stonex, GeoSLAM and TLS. A statistically significant difference was found between the FSCT and 3DFin algorithms, software has the biggest impact on TH errors, which shows the importance of proper data processing. In the case of the TH assessment, the iPhone was not considered, due to the low range of the LiDAR sensors, which prevents the derivation of TH (Table 4).

The results highlight differences in the estimated marginal TH means across the three device types (Geo-

Table 3. Linear regression of estimation error on reference diameter at breast height with device interactions.

	Estimate	Std. Error	t value	p value
Intercept	0.175	0.186	0.94	0.347
Reference DBH	–0.06	0.008	–7.89	<0.001***
Device: iPhone	3.481	0.266	13.09	<0.001***
Device: Stonex	2.015	0.263	7.67	<0.001***
Device: TLS	–0.145	0.263	–0.55	0.582
Reference DBH × iPhone	–0.026	0.011	–2.43	0.015*
Reference DBH × Stonex	–0.002	0.011	–0.23	0.821
Reference DBH × TLS	0.031	0.011	2.87	0.004**

Notes: Significant Codes 0 0.001 '***' 0.01 '**' 0.05 '*' 0.1 '.' Model fit: $R^2 = 0.219$, $p < 0.001$.

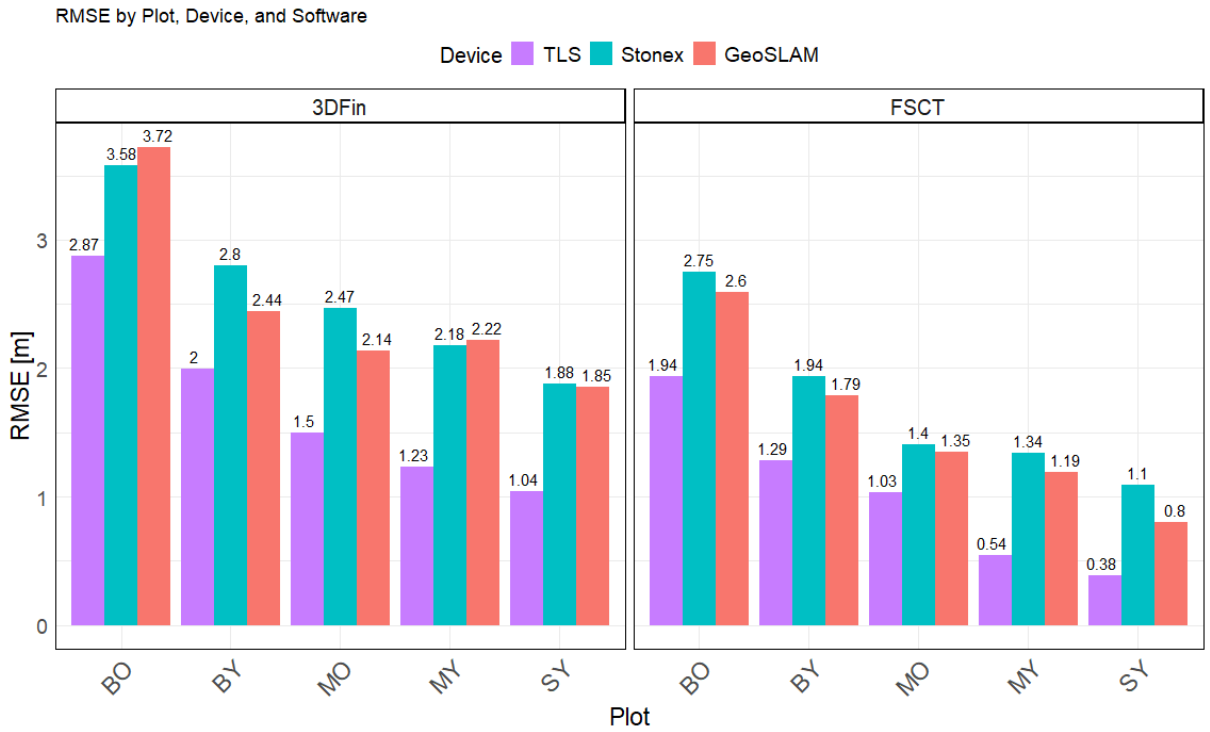

Fig. 7. Root mean square error for tree height. Bar plots show RMSE: Left 3DFin based, right FSCT based (BY – beech young, BO – beech old, SY – spruce young, MY – mixture young, MO – mixture old).

SLAM, Stonex, and TLS), analysed for two types of analyses (3DFin and FSCT) (Fig. 8). 3DFin has larger error ranges (±3.5 m) compared to FSCT (±1.5 m), indicating that FSCT is the more accurate algorithm. The TLS using FSCT algorithm demonstrated the most precise measurements, as it consistently exhibited the lowest deviations from the reference tree heights. The smallest absolute errors (not statistically significant) were observed for SY and MY using FSCT algorithm, suggesting that this combination yielded the most reliable results. In contrast, GeoSLAM and Stonex with 3DFin algorithm produced systematically larger negative errors, indicating a general underestimation of tree height. Among these, Stonex (3DFin) for BO and BY had the largest errors (–3.0 m and –2.7 m, respectively).

Error distribution analysis shows that FSCT generally achieves smaller error and more stable results than 3DFin for tree height (Appendix A4). The differences between devices (TLS, Stonex, GeoSLAM) are often smaller than the difference caused by the software itself, although we see a larger error variance for TLS in some stands with 3DFin. For older stands (BO, MO) the number of outliers increases, indicating the influence of more complex tree structure on height estimation. Overall, this shows that the choice of algorithm (FSCT vs. 3DFin) plays a key role in TH estimation and that FSCT shows greater accuracy and less error variance.

4. Discussion

4.1. Influence of the device

The results of the analysis of variance showed that the most significant factor influencing DBH is the device. In general, the results show that the most accurate device for DBH estimation is TLS. This finding is consistent with the claims of several authors (Liang et al. 2018; Mokroš et al. 2021; Stal et al. 2021; Kükenbrink et al. 2022). There are several studies on the use of the Faro scanner in forest environments. Bauwens et al. (2016) achieved RMSE

Table 4. Analysis of variance results for tree height. The table presents degrees of freedom (Df), sum of squares (Sum Sq), mean square (Mean Sq), F-value, and associated p-value for the tested effects.

TH	Df	Sum Sq	Mean Sq	F value	p-value	
Device	2	20	10.23	4.461	0.232870	
Plot	4	90	22.53	3.216	0.012560	*
Tree	1	90	89.87	12.827	0.000369	***
Software	1	149	149.19	21.293	4.8e-06	***
Residuals	615	4309	7.01			
Significant Codes	0	0.001 '***'	0.01 '**'	0.05 '*'	0.1 '.'	

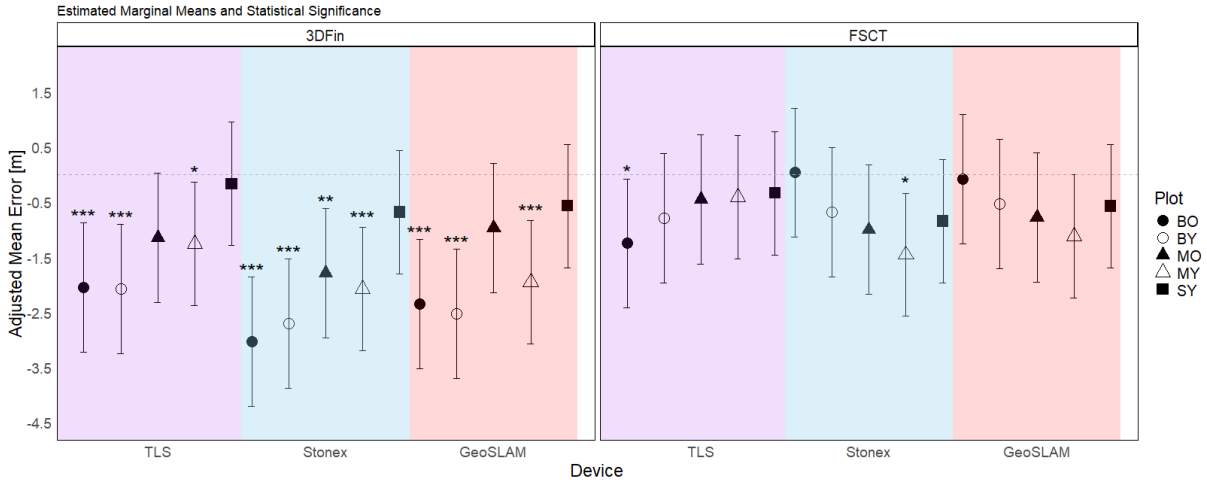

Fig. 8. REstimated Marginal Means of tree height according to each device used, and different sites and algorithm. Significant differences between estimated and reference (TH), according to each device used, different sites and algorithm, are indicated as follows: 0.001 '***', 0.01 '**', 0.05 '*'.

3.73 cm or Kükenbrink et al. (2022) achieved RMSE 1.6 cm. In case of this study (Fig. 5.), the RMSE reached the range from 1.2 cm (BO; 3DFin) to 2.7 cm (SY; FSCT).

When considering TH, the most significant factor influencing it is the algorithm. The results subsequently showed the influence of the tree species. The impact of the device on the accuracy of TH derivation has not been proven. The most accurate device for TH estimation is TLS (Cabo et al. 2018a). Several studies using TLS point clouds for TH estimation have compared TLS-derived values with field measurements. For example, one study (Wang et al. 2019) reported an overall RMSE of 1.68 m in easy plots and 2.11 m in difficult plots, while another (Liu et al. 2018) found an average TH RMSE of 0.95 m. In our study (Fig. 6), the RMSE ranged from 0.42 m (SY, FSCT) to 6.38 m (BO, 3Dfin).

Among the tested devices, TLS provided the highest accuracy but required substantially more effort and cost. In our experiment, data collection from 13 TLS positions on a 30 × 30 m plot took about 2.5 hours, compared to just 4 minutes with HMLS. TLS devices are expensive, demand considerable post-processing time, and require skilled operators, as errors in acquisition can strongly affect point cloud quality. Despite its robustness and accuracy, the high costs and labour-intensive scanning limit the feasibility of TLS for national forest inventories (Kükenbrink et al. 2022). The second most accurate device for DBH estimation was HMLS. In this study, we tested two HMLS that differ mainly in their price. Device prices were obtained from local Slovak distributors for educational institutions. Despite large price differences, the devices showed comparable performance, with no statistically significant differences in DBH estimates. In HMLS the trajectory used for data collection is very important (Mokroš et al. 2021). In this study we have used the trajectory that has been shown to be the best in previous studies (Chudá et al. 2024). Although no one has tested the accuracy of the HMLS Stonex X102GO in a forest environment, there are several studies on the HMLS Zeb Horizon. For example, reference (Tupinambá-Simões et al. 2023) reported RMSE 1.9 cm (*Pinus pinaster* Aiton) to 3.7 cm (*Quercus pyrenaica* Willd.), while (Mokroš et al. 2021) demonstrated that Zeb Horizon achieved an RMSE of 6.3 cm across plots with varying density. In our study (Fig. 5), the RMSE for Stonex ranged from 1.5 cm (BO; FSCT) to 3.9 cm (SY; FSCT), and for GeoSLAM it ranged from 1.8 cm (BO; FSCT) to 4.3 cm (SY; FSCT).

The points dispersion was clearly higher in point clouds from HMLSs (Appendix A5). This mainly influenced DBH estimation, while TH was only secondarily affected, with the algorithm having a stronger impact. Although there are often TH underestimation caused by ground-based laser scanning systems, e.g., TLS or WLS encompassing HMLSs (Cabo et al. 2018a; Liang et al. 2018) the effect of the device on the determination of TH has been shown to be insignificant.

Clearly, the lowest accuracy in DBH estimation was achieved with the iPhone, which exhibited the highest error across all research plots RMSE has achieved a range from 2.732 cm (BY; FSCT) to 6.726 cm (BY; 3DFin). This is consistent with the authors' claims DBH RMSE 3.14 cm in (Mokroš et al. 2021). Some studies report better results, such as an DBH RMSE of 0.963 cm for the iPhone and 0.961 cm for the iPad using the ForestScanner app (Tatsumi et al. 2022). However, these results may be attributed to more favourable conditions, as the study was conducted in a plot with almost no understory vegetation. Results comparable to this study were also achieved by study (McGlade et al. 2023), which reported an RMSE 3.13 cm for continuous capture of native woodlands using Apple iPad Pro 2020. Additionally, one limitation of these devices is their limited scanning range.

The main advantage of the iPhone LiDAR is its speed and affordability. Its key limitation is the 5 m range,

which restricts scanning to tree trunks and prevents TH estimation by excluding crowns (Mokroš et al. 2021). As the studied stands exceeded this range, the device's impact on TH determination could not be assessed.

Overall, it is essential for anyone wishing to acquire data using LiDAR-based methods to first determine the required level of accuracy they need and the financial resources they are willing to allocate. In today's world of advanced technology, HMLS like GeoSLAM or Stonex are sufficient for routine forest ecosystem monitoring and forestry planning. However, for more detailed analyses, such as measuring tree growth or using quantitative structure models to estimate above-ground biomass (Calders et al. 2015), from ground based methods TLS is necessary. Conversely, if the priority is quick, simple, and efficient forest monitoring with minimal data usage, the iPhone LiDAR is a suitable alternative. Despite its limited range, it remains well-suited for a wide variety of tasks.

4.2. Influence of the plot

The second most important factor affecting DBH estimation was the plot, influenced by tree species and stem thickness. The largest RMSE occurred in young, thin spruces, whose low branches distorted DBH measurements (Appendix A6). Errors occurred mainly at 1.3 m height, as confirmed by checking cross-sections with the highest RMSE, where branches or neighbouring stems interfered with measurements.

In this study, DBH RMSE ranged from 1.2 cm (SY; TLS) to 1.9 cm (MO; TLS) for 3DFin, and from 1.2 cm (BO; TLS) to 2.7 cm (SY; TLS) for FSCT (Fig. 6). Similar values were reported by (Mokroš et al. 2021), who achieved an RMSE of 1.5 cm with the Faro Focus S70, and by (Kükenbrink et al. 2022), who found an RMSE of 1.6 cm for TLS in temperate forests. Liang et al. (2018) also confirmed that plot conditions strongly influence DBH accuracy, with higher RMSE in more complex stands. Our results are therefore consistent with previous findings. In older stands, HMLS can provide reliable DBH estimates where branches are absent due to closed canopies, while iPhone LiDAR may also achieve sufficiently low RMSE for some applications. By contrast, in younger stands its limited range complicates data collection and increases error rates.

Tukey's HSD test showed statistically significant differences in TH errors between SY and BO (mean difference 0.93, CI 0.01–1.84, $p = 0.047$) and between SY and BY (mean difference 1.03, CI 0.11–1.95, $p = 0.019$), with SY exhibiting more errors in both cases. Other comparisons (e.g., MY vs. MO, BY vs. BO) were not significant ($p > 0.05$). These results indicate that age and species affect TH errors, with young conifers differing significantly from deciduous groups.

Our analysis demonstrated that DBH estimation error was indeed influenced by tree size, but the magnitude and direction of this effect differed among devices. In general, smaller stems were more prone to overestimation, whereas accuracy improved with increasing DBH. This pattern was particularly pronounced for the iPhone, which exhibited strong overestimation in small stems that diminished as stem diameter increased. Stonex also showed systematic overestimation, but its size-related trend did not significantly differ from GeoSLAM, indicating that its errors were more uniform across tree sizes. TLS, in contrast, was nearly unbiased for smaller stems but exhibited a shallower error decline, leading to slight underestimation of larger trees. When evaluating the factors affecting measurement accuracy, it is also important to consider additional sources of error. Understory vegetation is a well-known source of error in tree height estimation, as it can occlude treetops and complicate the detection of the highest crown point (Liang et al. 2018). In the present study, this factor was excluded by selecting plots without significant understory, since the primary objective was to assess different influencing factors. Nevertheless, we acknowledge that in operational settings understory can substantially influence measurement accuracy, and its effect will be explicitly addressed in future research phases.

Building on this, practical recommendations can be made for monitoring strategies in different stand types. For detailed monitoring of the young stands, it is recommended to use more accurate technologies, ideally TLS with FSCT, but assuming that results with lower accuracy are sufficient, HMLS can be effectively used, provided that scanning paths and angles are planned to capture the canopy tops, which is often feasible in young, lower-height stands.

4.3. Influence of the algorithm

Our results show that the choice of software (FSCT or 3DFin) had no significant effect on DBH error, as supported by the large p-value. Similarly, the international TLS benchmarking study (Liang et al. 2018), tested fourteen algorithms that differed in design, workflow, and parameter settings, yet all were highly automated and produced comparable outcomes. The algorithms differed in development methods, data structure, and parameter settings, yet all were highly automated. Reported RMSE values ranged from 2–4 cm for robust algorithms and 1–3 cm for conservative ones. Although algorithm type was not directly tested here, many approaches produced stable RMSE across plot conditions (easy, medium, difficult), which our ANOVA confirmed (Table 2). For example, DBH RMSE at difficult plots exceeded 3 cm for the TUDelft and RILOG algorithms (Liang et al. 2018). Conversely, the FGI and TreeMetrics algorithms

consistently maintained RMSE below 1 cm throughout the entire experiment (Liang et al. 2018). In contrast, FSCT and 3Dfin are relatively new algorithms, but they are faster than other algorithms and consistently give good results with unchanged parameters. In case of this study across the five various plot conditions and four different devices, the RMSE was 2.63 cm for 3DFin and 2.83 cm for FSCT, and a significant impact on the size of the error is due to stands with complicated structure.

Unlike DBH, TH estimation was strongly affected by the choice of software (FSCT or 3DFin), confirming that the derivation algorithm has the largest impact on TH errors. Improving TH accuracy therefore requires careful software selection and consideration of species- and plot-specific differences. As it was mentioned before, to calculate the TH, FSCT integrates the measurements of the cylindrical segments representing the trunk with the vegetation points associated with each tree and the highest point from these combined data is then chosen as the TH (Krisanski et al. 2021), which is proving to be a more efficient approach. 3Dfin collects points around the calculated trunk axis, subsequently voxelizes the cloud, clusters the voxels, sorts and removes small clusters – noise. Voxels further than a certain threshold from the tree axis are discarded and then the normalized Z value of the highest remaining voxel is used as TH (Laino et al. 2024). We assume FSCT manages canopy noise more effectively due to its method of TH determination, while 3DFin is less accurate when parameters are predefined. A second issue was that 3DFin sometimes assigned the TH of a taller neighboring tree to the target. The results indicate that FSCT outperforms 3DFin on the metric under study.

As already pointed out in the previous sections of this paper, there are significant differences in the DBH estimation approach between FSCT and 3DFin. FSCT uses the lowest diameter of the tree to find the DBH and vertically projects it onto the DTM. This assumes that although occlusion is common in point clouds from the forest environment, it is a safe assumption that the tree is connected to the ground and at the same time its base is approximately straight downwards. The DBH – nominally 1.3 m above the ground – in FSCT is calculated by taking the mean diameter and X, Y position of all cylinder measurements between 1.0 m and 1.6 m above the DTM on a per tree basis. This means that even if the lower section of the tree is missing, FSCT will use higher up cylinder measurements, which have been projected to the ground, as the DBH measurement (Krisanski et al. 2021). In contrast the computation of DBH in 3DFin is based on circle fitting to the identified stem through least-squares minimization. To identify the stems, the limbing algorithm is applied to every tree to remove branches, the whole stems are identified along tree axes and finally optimal circle algorithm is used to extract DBHs at 1.3 m (Laino et al. 2024). From a practical perspective, errors in DBH are more critical for volume and biomass estimation than errors in tree height, because volume calculations depend on DBH squared or cubed, amplifying any measurement inaccuracies. Therefore, precise DBH estimation is essential for accurate forest inventory results (Avery & Burkhart 2015).

With unchanged parameters, 3DFin applies optimal circle fitting, which appears more effective than the cylinder fitting used by FSCT. Its main advantage, however, is processing speed: while FSCT required about 7 hours per plot, 3DFin processed the same data in only 10 minutes. 3DFin is also easier to use, being integrated into CloudCompare, whereas FSCT runs as a Python script and requires programming skills, which may limit its practical adoption.

The choice of tool ultimately lies with the user. In our case, 3DFin provided better results and was significantly faster than FSCT, as it is directly integrated into CloudCompare, making it easier to use. However, 3DFin does not offer as wide a range of calculations as FSCT. In contrast to 3DFin, FSCT offers a number of outputs that can be exported separately to the source directory for example cleaned segmented point cloud created during the post-processing step, digital terrain model in point form, vegetation points, ground vegetation points, stem points, stem points assigned by tree ID, a point cloud text visualisation and many other outputs. For forest management planning, 3DFin is sufficient and easy to use, yet for scientific purposes or extensive analysis, FSCT is more suitable. It was demonstrated, that 3DFin generally outperforms FSCT, as shown consistently higher R^2 and a lower average RMSE values across the most plots, indicating it provides more accurate DBH estimation. On the other hand, some plots / tree species pose challenges for both methods, particularly FSCT, suggesting the need for improvements or adjustments when applied in those challenging environment.

5. Conclusions

In the manuscript we presented a comparison of different devices for the making of 3D point clouds in different conditions, evaluated by different algorithms. We examined key factors influencing DBH and TH estimation by comparing widely used devices (TLS FARO Focus 3D S150, HMLS Stonex X120GO SLAM and GeoSLAM ZEB Horizon, and iPhone 13 Pro Max LiDAR) across plots with varying densities and species compositions, using two advanced algorithms (FSCT and 3DFin).

The results showed that the device used has the greatest influence on the resulting DBH estimation. TLS achieved the highest DBH accuracy, while iPhone performed worst. HMLS devices (Stonex, GeoSLAM) showed no significant differences despite their price gap.

Species also influenced errors, with young spruce most affected due to branches at breast height. The choice of algorithm had no significant impact on DBH estimation.

In TH evaluation, the algorithm used has the greatest impact on the error. FSCT shows significantly lower errors compared to 3DFin, which highlights the importance of proper data processing. HMLS devices Stonex and GeoSLAM achieve similar errors, with TLS showing the lowest estimation error in all cases. For TH, iPhone was not included in the analysis due to the limited range of the LiDAR sensor, which does not allow for TH determination. TH errors were highest in older stands and more pronounced in deciduous than in coniferous species. Tukey's HSD confirmed significant differences between FSCT and 3DFin and between spruce and beech, underscoring the importance of selecting appropriate algorithms and devices.

Thus, both 3DFin and FSCT can be used to estimate DBH and TH from point clouds. Each algorithm has its own advantages and disadvantages (Appendix A7).

FSCT, though slower and requiring programming skills, provides more detailed outputs, including better TH accuracy. In contrast, 3DFin is faster and easier to use within CloudCompare but offers fewer parameters. The choice depends on whether users prioritize detail and accuracy (FSCT) or speed and simplicity (3DFin). The optimal choice of device and algorithm depends on the application. For detailed monitoring requiring high spatial resolution, such as crown analysis or microhabitat studies, TLS is most suitable.

TLS highly detailed point clouds capture even the thin forest details with exceptional precision, although the process is time-consuming and demands considerable expertise in data collection and post-processing. Conversely, HMLS devices (such as GeoSLAM ZEB Horizon and Stonex X120GO) provide a robust alternative for routine forest management tasks. They deliver nearly comparable accuracy in estimating DBH and tree height, yet they require less time for data acquisition and incur lower costs, making them well suited for operational applications where efficiency is of utmost importance. Finally, while smartphone-based LiDAR (e.g., iPhone 13 Pro Max) offers rapid data collection and affordability, its limited scanning range means it is best suited for quick, preliminary assessments of forest characteristics rather than detailed inventory tasks.

Therefore, when selecting the appropriate approach, it is important to consider whether high accuracy (TLS), speed and mobility (MLS) or low cost and ease of use (iPhone LiDAR) are more important. If the goal is to obtain detailed outputs with higher accuracy in determining tree height, it is advisable to reach for the FSCT, although it requires longer processing time and more demanding control. Conversely, 3DFin allows faster processing and easier operation, but may have a slightly higher error rate when calculating TH. In terms of the selection of the devices themselves, TLS represents the most accurate, but the most expensive and time-consuming solution (Appendix A8). The HMLS offers a balanced compromise between price, accuracy and time efficiency, while the iPhone LiDAR is affordable and very fast in data collection, but its limited range and lower accuracy make it more suitable for quick orientation measurements or monitoring in smaller forest stands. Overall, the final choice of device and algorithm depends on whether high accuracy, speed and ease of use or cost is key for the user.

Acknowledgements

The paper was funded by the EU NextGenerationEU through the Recovery and Resilience Plan for Slovakia under the project No. 09I03-03-V04-00341.

References

Astrup, R., Ducey, M. J., Granhus, A., Ritter, T., von Lüpke, N., 2014: Approaches for estimating stand-level volume using terrestrial laser scanning in a single-scan mode. Canadian Journal of Forest Research, 44:666–76.

Avery, T. E., Burkhart, H. E., 2015: Forest Measurements: Fifth Edition. Long Grove, Illinois, Waveland Press, 456 p.

Balenović, I., Liang, X., Jurjević, L., Hyyppä, J., Seletković, A., Kukko, A., 2021: Hand-Held Personal Laser Scanning: Current Status and Perspectives for Forest Inventory Application. Croatian journal of forest engineering, 42:165–83.

Bauwens, S., Bartholomeus, H., Calders, K., Lejeune, P., 2016: Forest inventory with terrestrial LiDAR: A comparison of static and hand-held mobile laser scanning. Forests, 7:127.

Binot, J.-M., Pothier, D., Lebel, J., 1995: Comparison of Relative Accuracy and Time Requirement between the Caliper, the Diameter Tape and an Electronic Tree Measuring Fork. The Forestry Chronicle, 71:197–200.

Cabo, C., Del Pozo, S., Rodríguez-Gonzálvez, P., Ordóñez, C., González-Aguilera, D., 2018a: Comparing terrestrial laser scanning (TLS) and wearable laser scanning (WLS) for individual tree modeling at plot level. Remote Sensing, 10:540.

Cabo, C., Ordóñez, C., López-Sánchez, C. A., Armesto, J., 2018b: Automatic Dendrometry: Tree Detection, Tree Height and Diameter Estimation Using Terrestrial Laser Scanning. International Journal of Applied Earth Observation and Geoinformation, 69:164–174.

Calders, K., Newnham, G., Burt, A., Murphy, S., Raumonen, P., Herold, M. et al., 2015: Nondestructive Estimates of Above-Ground Biomass Using Terrestrial Laser Scanning. Methods in Ecology and Evolution, 6:198–208.

Gollob, C., Ritter, T., Nothdurft, A., 2020: Forest Inventory with Long Range and High-Speed Personal Laser Scanning (PLS) and Simultaneous Localization and Mapping (SLAM) Technology. Remote Sensing, 12:1509.

Gollob, C., Ritter, T., Kraßnitzer, R., Tockner, A., Nothdurft, A., 2021: Measurement of Forest Inventory Parameters with Apple iPad Pro and Integrated LiDAR Technology. Remote Sensing, 13:3129.

Guenther, M., Heenkenda, M. K., Morris, D., Leblon, B., 2024: Tree Diameter at Breast Height (DBH) Estimation Using an iPad Pro LiDAR Scanner: A Case Study in Boreal Forests, Ontario, Canada. Forests, 15:214.

Hyyppä, E., Kukko, A., Kaijaluoto, R., White, J. C., Wulder, M. A., Pyorala, J. et al., 2020: Accurate Derivation of Stem Curve and Volume Using Backpack Mobile Laser Scanning. ISPRS Journal of Photogrammetry and Remote Sensing, 161:246–262.

Hyyppä, E., Yu, X., Kaartinen, H., Hakala, T., Kukko, A., Vastaranta, M. et al., 2020: Comparison of backpack, handheld, under-canopy UAV, and above-canopy UAV laser scanning for field reference data collection in boreal forests. Remote Sensing, 12:1–31.

Chen, S., Liu, H., Feng, Z., Shen, C., Chen, P., 2019: Applicability of Personal Laser Scanning in Forestry Inventory. PLoS ONE, 14:e0211392.

Chudá, J., Výbošťok, J., Tomaštík, J., Chudý, F., Tunák, D., Skladan, M. et al., 2024: Prompt Mapping Tree Positions with Handheld Mobile Scanners Based on SLAM Technology. Land, 13:93.

Krause, S., Sanders, T. G. M., Mund, J.-P., Greve, K., 2019: UAV-Based Photogrammetric Tree Height Measurement for Intensive Forest Monitoring. Remote Sensing, 11:758.

Krisanski, S., Taskhiri, M. S., Aracil, S. G., Herries, D., Muneri, A., Gurung, M. B. et al., 2021: Forest structural complexity tool – an open source, fully-automated tool for measuring forest point clouds. Remote Sensing, 13:4677.

Kükenbrink, D., Marty, M., Bösch, R., Ginzler, C., 2022: Benchmarking Laser Scanning and Terrestrial Photogrammetry to Extract Forest Inventory Parameters in a Complex Temperate Forest. International Journal of Applied Earth Observation and Geoinformation, 113:102999.

Laino, D., Cabo, C., Prendes, C., Janvier, R., Ordonez, C., Nikonovas, T. et al., 2024: 3DFin: a software for automated 3D forest inventories from terrestrial point clouds. Forestry: An International Journal of Forest Research, 97:479–496.

Larjavaara, M., Muller-Landau, H. C., 2013: Measuring Tree Height: A Quantitative Comparison of Two Common Field Methods in a Moist Tropical Forest. Methods in Ecology and Evolution, 4:793–801.

Li, J., Yang, B., Yang, Y., Zhao, X., Liao, Y., Zhu, N. et al., 2023: Real-Time Automated Forest Field Inventory Using a Compact Low-Cost Helmet-Based Laser Scanning System. International Journal of Applied Earth Observation and Geoinformation, 118:103299.

Li, J., Yuan, S., Cao, M., Nguyen, T.-M., Cao, K., Xie., L., 2024: HCTO: Optimality-Aware LiDAR Inertial Odometry with Hybrid Continuous Time Optimization for Compact Wearable Mapping System. arXiv:2403.14173.

Liang, X., Hyyppä, J., Kukko, A., Kaartinen, H., Jaakkola, A., Yu, X., 2014: The Use of a Mobile Laser Scanning System for Mapping Large Forest Plots. IEEE Geoscience and Remote Sensing Letters, 11:1504–1508.

Liang, X., Kankare, V., Hyyppä, J., Wang, Y., Kukko, A., Haggrén, H. et al., 2016: Terrestrial Laser Scanning in Forest Inventories. ISPRS Journal of Photogrammetry and Remote Sensing, Theme issue "State-of-the-art in photogrammetry, remote sensing and spatial information science", 115:63–77.

Liang, X., Hyyppä, J., Kaartinen, H., Lehtomäki, M., Pyörälä, J., Pfeifer, N. et al., 2018: International Benchmarking of Terrestrial Laser Scanning Approaches for Forest Inventories. ISPRS Journal of Photogrammetry and Remote Sensing, 144:137–179.

Liu, G., Wang, J., Dong, P., Chen, Y., Liu, Z., 2018: Estimating Individual Tree Height and Diameter at Breast Height (DBH) from Terrestrial Laser Scanning (TLS) Data at Plot Level. Forests, 9:398.

Luoma, V., Saarinen, N., Wulder, M., White, J., Vastaranta, M., Holopainen, M. et al., 2017: Assessing Precision in Conventional Field Measurements of Individual Tree Attributes. Forests, 8:38.

Martin, A., 2022: Accuracy and Precision in Urban Forestry Tools for Estimating Total Tree Height. Arboriculture & Urban Forestry, 48:319–332.

McGlade, J., Wallace, L., Hally, B., Reinke, K., Jones, S., 2023: The Effect of Surrounding Vegetation on Basal Stem Measurements Acquired Using Low-Cost Depth Sensors in Urban and Native Forest Environments. Sensors, 23:3933.

Mokroš, M., Mikita, T., Singh, A., Tomaštík, J., Chudá, J., Wężyk, P. et al., 2021: Novel Low-Cost Mobile Mapping Systems for Forest Inventories as Terrestrial Laser Scanning Alternatives. International Journal of Applied Earth Observation and Geoinformation, 104:102512.

Ritter, T., Gollob, C., Nothdurft, A., 2020: Towards an Optimization of Sample Plot Size and Scanner Position Layout for Terrestrial Laser Scanning in Multi-Scan Mode. Forests, 11:1099.

Rouzbeh Kargar, A., MacKenzie, R. A., Apwong, M., Hughes, E., Van Aardt, J., 2020: Stem and Root Assessment in Mangrove Forests Using a Low-Cost, Rapid-Scan Terrestrial Laser Scanner. Wetlands Ecology and Management, 28:883–900.

Ryding, J., Williams, E., Smith, M. J., Eichhorn, M. P., 2015: Assessing handheld mobile laser scanners for forest surveys. Remote Sensing, 7:1095–1111.

Saliu, I. S., Satyanarayana, B., Bin Fisol, M. A., Wolswijk, G., Decannière, C., Lucas, R. et al., 2021: An Accuracy Analysis of Mangrove Tree Height Mensuration Using Forestry Techniques, Hypsometers and UAVs. Estuarine, Coastal and Shelf Science, 248:106971.

Skladan, M., Chudá, J., Singh, A., Masný, M., Lieskovský, M., Pástor, M. et al., 2025: Choosing the Right Close-Range Technology for Measuring DBH in Fast-Growing Trees Plantations. Trees, Forests and People, 19:100747.

Stal, C., Verbeurgt, J., De Sloover, L., De Wulf, A., 2021: Assessment of Handheld Mobile Terrestrial Laser Scanning for Estimating Tree Parameters. Journal of Forestry Research, 32:1503–1513.

Tatsumi, S., Yamaguchi, K., Furuya, N., 2022: ForestScanner: A Mobile Application for Measuring and Mapping Trees with LiDAR-Equipped iPhone and iPad. Methods in Ecology and Evolution. Special Feature: Active Remote Sensing for Ecology and Ecosystem Conservation, 14:1603–1609.

Tupinambá-Simões, F., Pascual, A., Guerra-Hernández, J., Ordóñez, C., de Conto, T., Bravo, F., 2023: Assessing the Performance of a Handheld Laser Scanning System for Individual Tree Mapping – A Mixed Forests Showcase in Spain. Remote Sensing, 15:1169.

Wang, Y., Lehtomäki, M., Liang, X., Pyörälä, J., Kukko, A., Jaakkola, A. et al., 2019: Is Field-Measured Tree Height as Reliable as Believed – A Comparison Study of Tree Height Estimates from Field Measurement, Airborne Laser Scanning and Terrestrial Laser Scanning in a Boreal Forest. ISPRS Journal of Photogrammetry and Remote Sensing, 147:132–145.

Wardius, Y., Hein, S., 2024: Terrestrial Laser Scanning vs. Manual Methods for Assessing Complex Forest Stand Structure: A Comparative Analysis on Plenter Forests. European Journal of Forest Research, 143:635–649.

Wilkes, P., Lau, A., Disney, M., Calders, K., Burt, A., Gonzalez de Tanago, J. et al., 2017: Data Acquisition Considerations for Terrestrial Laser Scanning of Forest Plots. Remote Sensing of Environment, 196:140–153.

Other sources

"Files: Anaconda.org". n.d. Cit 18. august 2023. Available at https://anaconda.org/anaconda/anaconda-navigator/files?version=2.4.0&page=0.

Appendix A

Appendix A1. Relationship between reference diameter at the breast height (DBH) and estimated DBH for each forest plot, comparing four devices (TLS, GeoSLAM, Stonex, iPhone) under both 3DFin and FSCT algorithms.

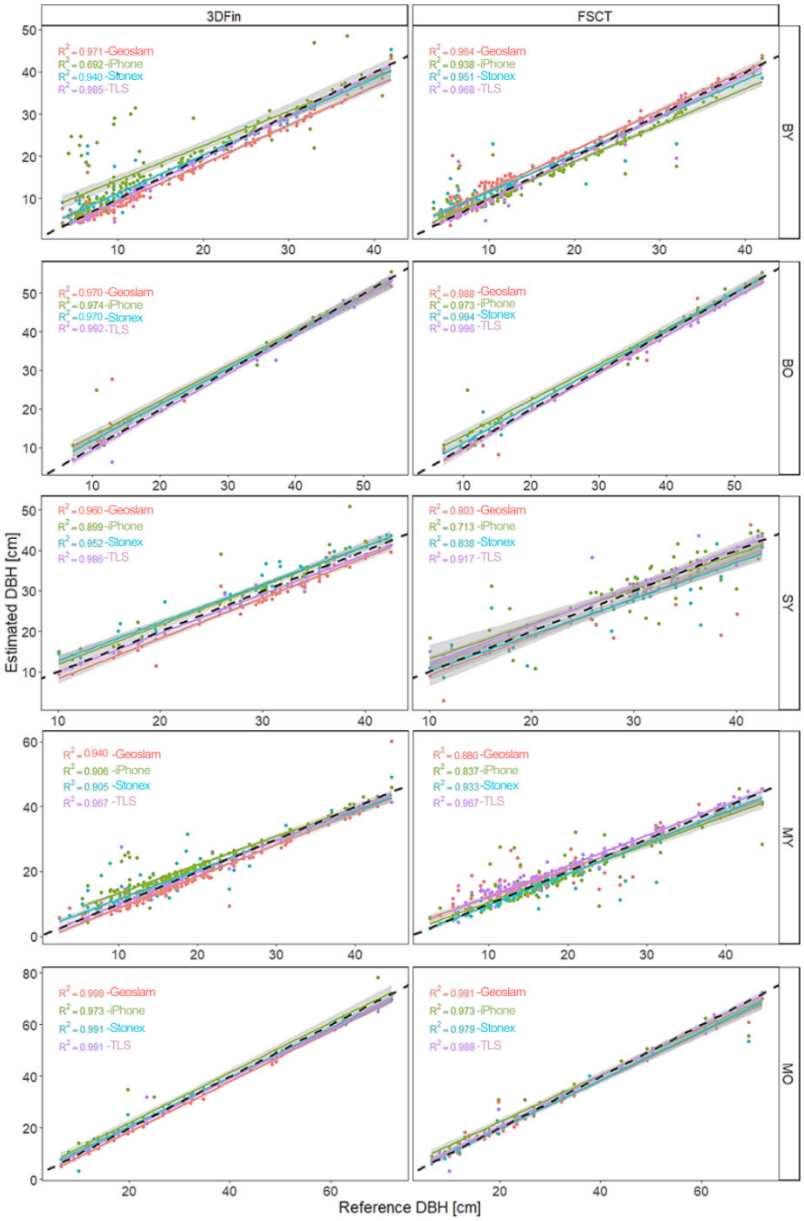

Appendix A2.

A2.1. Regression Analysis for Diamteter at the Breast Height Estimation.

Tree DBH

Device	Plot	Algorithm	R^2	RMSE (cm)	rRMSE (%)	Ref_{min} (cm)	Ref_{max} (cm)	Ref_{mean} (cm)	Ref_{sd} (cm)	Est_{min} (cm)	Est_{max} (cm)	Est_{mean} (cm)	Est_{sd} (cm)	n	$Error_{min}$ (cm)	$Error_{max}$ (cm)	$Error_{sd}$ (cm)	Bias (cm)
TLS	BY	3DFin	0.985	1.314	8.345	3.50	42.00	15.75	10.23	4.00	43.94	15.29	10.23	128	−5.14	11.50	1.237407286	−0.457
		FSCT	0.968	1.848	11.731	3.50	42.00	15.75	10.15	4.00	41.70	15.43	10.15	128	−12.50	12.30	1.826886439	−0.320
	BO	3DFin	0.992	1.629	5.730	7.10	54.10	28.42	15.80	6.29	53.35	27.61	15.80	40	−6.61	1.07	1.433661987	−0.815
		FSCT	0.996	1.237	4.352	7.10	54.10	28.42	15.53	9.40	52.80	27.67	15.53	40	−2.30	2.40	0.994480737	−0.756
	SY	3DFin	0.986	1.246	4.295	10.10	42.50	29.02	8.26	9.83	41.27	28.28	8.26	52	−4.21	2.91	1.013455514	−0.738
		FSCT	0.917	2.692	9.277	10.10	42.50	29.02	8.44	14.20	43.70	28.56	8.44	52	−3.50	12.30	2.470906321	−0.456
	MY	3DFin	0.967	1.679	9.098	2.50	44.60	18.45	9.08	2.40	42.13	18.23	9.08	142	−3.30	17.04	1.671034192	−0.614
		FSCT	0.967	2.431	13.176	2.50	44.60	18.45	8.53	4.40	45.60	20.58	8.53	142	−2.70	9.40	1.642866405	0.320
	MO	3DFin	0.991	1.959	6.572	6.50	72.10	29.80	18.31	5.97	71.26	29.19	18.31	34	−4.39	8.53	1.887619549	−0.614
		FSCT	0.988	2.084	6.992	6.50	72.10	29.80	18.57	3.30	72.60	30.12	18.57	34	−6.60	7.40	2.089159696	0.320
Stonex	BY	3DFin	0.940	2.608	16.556	3.50	42.00	15.75	9.51	4.94	45.31	16.43	9.51	128	−3.75	16.09	2.52586581	0.684
		FSCT	0.951	2.510	15.936	3.50	42.00	15.75	9.21	5.80	41.00	16.64	9.21	128	−9.00	12.40	2.355325149	0.892
	BO	3DFin	0.970	2.839	9.988	7.10	54.10	28.42	15.04	10.16	51.84	28.95	15.04	40	−2.26	14.72	2.832268839	0.533
		FSCT	0.994	1.473	5.183	7.10	54.10	28.42	15.49	8.60	53.70	29.12	15.49	40	−2.40	6.30	1.320297498	0.694
	SY	3DFin	0.952	2.478	8.538	10.10	42.50	29.02	8.18	13.01	43.79	30.69	8.18	52	−1.46	6.94	1.84856854	1.671
		FSCT	0.838	3.870	13.335	10.10	42.50	29.02	8.25	8.60	43.40	27.18	8.25	52	−15.00	9.60	3.436350093	−1.843
	MY	3DFin	0.905	2.878	15.595	2.50	44.60	18.45	8.73	5.60	49.03	19.08	8.73	142	−9.50	13.50	2.819483536	0.625
		FSCT	0.933	2.463	13.349	2.50	44.60	18.45	9.04	2.40	42.60	17.74	9.04	142	−15.40	3.90	2.366602112	−0.713
	MO	3DFin	0.991	1.963	6.586	6.50	72.10	29.80	18.18	3.30	69.50	29.85	18.18	34	−6.60	5.40	1.990780135	0.049
		FSCT	0.979	2.951	9.902	6.50	72.10	29.80	18.05	6.00	71.80	28.96	18.05	34	−16.00	3.30	2.869544513	−0.843
GeoSLAM	BY	3DFin	0.971	2.318	14.716	3.50	42.00	15.75	9.43	4.02	43.23	14.32	9.43	128	−4.40	9.75	1.829448992	−1.433
		FSCT	0.964	2.564	16.277	3.50	42.00	15.75	9.86	3.60	43.90	17.65	9.86	128	−1.90	14.50	1.958455521	1.896
	BO	3DFin	0.970	2.839	9.988	7.10	54.10	28.42	15.04	10.16	51.84	28.95	15.04	40	−2.26	14.72	2.832268839	0.533
		FSCT	0.988	1.785	6.280	7.10	54.10	28.42	16.18	8.10	53.50	28.08	16.18	40	−7.10	4.00	1.780856988	−0.337
	SY	3DFin	0.960	2.433	8.386	10.10	42.50	29.02	8.63	9.35	42.25	27.29	8.63	52	−8.10	5.33	1.728006899	−1.730
		FSCT	0.803	4.350	14.989	10.10	42.50	29.02	8.95	2.90	46.40	27.22	8.95	52	−19.40	5.00	3.999099899	−1.800
	MY	3DFin	0.940	2.689	14.575	2.50	44.60	18.45	9.21	4.57	60.20	16.99	9.21	142	−14.60	15.60	2.262766703	−1.466
		FSCT	0.880	3.293	17.847	2.50	44.60	18.45	8.41	5.60	42.60	19.38	8.41	142	−10.80	13.60	3.171140888	0.929
	MO	3DFin	0.998	2.044	6.858	6.50	72.10	29.80	18.51	5.00	69.71	27.96	18.51	34	−3.91	0.15	0.903272296	−1.840
		FSCT	0.981	2.999	10.062	6.50	72.10	29.80	17.80	7.10	70.20	28.74	17.80	34	−8.60	10.30	2.844079801	−1.066
iPhone	BY	3DFin	0.692	6.726	42.705	3.50	42.00	15.75	10.07	3.90	48.55	19.25	10.07	128	−11.11	29.52	5.904526102	3.497
		FSCT	0.938	2.732	17.345	3.50	42.00	15.75	9.07	5.60	43.20	15.06	9.07	128	−14.40	10.70	2.652368162	−0.695
	BO	3DFin	0.974	3.042	10.703	7.10	54.10	28.42	14.66	10.70	55.52	29.81	14.66	40	−2.86	14.20	2.751479349	1.386
		FSCT	0.973	3.154	11.099	7.10	54.10	28.42	14.88	10.70	55.40	30.09	14.88	40	−2.70	14.20	2.717711843	1.672
	SY	3DFin	0.899	3.033	10.450	10.10	42.50	29.02	8.65	14.20	50.94	30.33	8.65	52	−1.91	13.20	2.763202845	1.307
		FSCT	0.713	4.758	16.397	10.10	42.50	29.02	8.63	10.80	44.90	29.62	8.63	52	−10.50	15.00	4.767473125	0.600
	MY	3DFin	0.906	3.506	18.999	2.50	44.60	18.45	8.28	4.40	45.85	20.96	8.28	142	−5.30	14.67	2.753155587	2.511
		FSCT	0.837	3.737	20.250	2.50	44.60	18.45	8.82	5.80	45.50	17.99	8.82	142	−16.20	16.10	3.72138582	−0.463
	MO	3DFin	0.973	3.475	11.661	6.50	72.10	29.80	18.75	7.65	78.33	31.45	18.75	34	−2.48	15.00	3.104629452	1.648
		FSCT	0.973	3.595	12.064	6.50	72.10	29.80	17.48	8.90	71.80	31.20	17.48	34	−13.70	11.10	3.361239767	1.397

A2.2. Regression Analysis for Tree Height Estimation.

Tree height

Device	Plot	Algorithm	R^2	RMSE (cm)	rRMSE (%)	Ref_{min} (m)	Ref_{max} (m)	Ref_{mean} (m)	Ref_{sd} (m)	Est_{min} (m)	Est_{max} (m)	Est_{mean} (m)	Est_{sd} (m)	n	$Error_{min}$ (m)	$Error_{max}$ (m)	$Error_{sd}$ (m)	Bias (m)
TLS	BY	3DFin	0.928	2.871	9.950	7.860	33.9	28.850	6.013	13.00	35.00	30.35	6.01	128	–1.08	8.56	2.510	1.50
		FSCT	0.972	1.941	6.727	7.860	33.9	28.850	6.815	13.00	38.00	30.10	6.81	128	0.07	5.14	1.521	1.25
	BO	3DFin	0.931	1.999	8.447	9.280	28.27	23.670	4.987	11.00	29.20	24.94	4.99	40	–1.34	3.80	1.588	1.27
		FSCT	0.961	1.285	5.431	9.280	28.27	23.670	5.747	10.58	32.00	24.32	5.75	40	–0.55	5.00	1.135	0.65
	SY	3DFin	0.817	1.496	5.040	22.520	35.54	29.673	3.034	23.00	35.22	30.43	3.03	52	–0.77	3.76	1.323	0.76
		FSCT	0.927	1.032	3.478	22.520	35.54	29.673	3.016	22.87	36.00	30.32	3.02	52	–0.18	3.39	0.822	0.65
	MY	3DFin	0.964	1.233	7.127	7.760	26.52	17.295	5.235	8.00	28.47	18.05	5.24	142	–0.45	3.09	0.998	0.75
		FSCT	0.997	0.543	3.138	7.760	26.52	17.295	5.089	8.23	26.74	17.70	5.09	142	–0.01	1.79	0.367	0.41
	MO	3DFin	0.926	1.039	4.531	12.580	28.37	22.920	3.774	12.84	28.64	23.16	3.77	34	–3.14	2.35	1.034	0.24
		FSCT	0.996	0.384	1.676	12.580	28.37	22.920	3.705	12.98	28.40	23.23	3.70	34	–0.24	0.70	0.228	0.31
Stonex	BY	3DFin	0.789	3.580	12.409	7.860	33.9	28.850	6.736	9.00	34.93	29.79	6.74	128	–5.51	9.87	3.544	0.94
		FSCT	0.916	2.753	9.543	7.860	33.9	28.850	6.831	14.00	39.00	30.44	6.83	128	–0.06	8.55	2.303	1.59
	BO	3DFin	0.830	2.802	11.838	9.280	28.27	23.670	4.926	11.00	29.54	25.25	4.93	40	–5.45	7.25	2.372	1.58
		FSCT	0.915	1.938	8.186	9.280	28.27	23.670	5.239	14.00	29.66	24.71	5.24	40	–5.00	4.72	1.678	1.04
	SY	3DFin	0.539	2.468	8.318	22.520	35.54	29.673	2.927	25.00	35.22	30.97	2.93	52	–1.55	8.81	2.157	1.29
		FSCT	0.907	1.405	4.734	22.520	35.54	29.673	2.843	23.45	35.80	30.76	2.84	52	–1.05	3.39	0.914	1.09
	MY	3DFin	0.939	2.176	12.584	7.760	26.52	17.295	5.164	8.41	27.59	19.05	5.16	142	–0.22	3.94	1.312	1.76
		FSCT	0.983	1.339	7.743	7.760	26.52	17.295	5.314	8.18	27.41	18.45	5.31	142	0.20	2.91	0.692	1.16
	MO	3DFin	0.766	1.882	8.212	12.580	28.37	22.920	3.363	14.72	28.70	23.56	3.36	34	–2.58	4.82	1.810	0.64
		FSCT	0.964	1.095	4.778	12.580	28.37	22.920	3.789	14.20	29.10	23.76	3.79	34	–1.52	1.78	0.714	0.84
GeoSLAM	BY	3DFin	0.823	3.724	12.908	7.860	33.9	28.850	5.594	15.00	34.03	30.26	5.59	128	–3.25	9.59	3.537	1.41
		FSCT	0.941	2.596	8.997	7.860	33.9	28.850	6.212	13.31	34.09	30.21	6.21	128	–0.64	10.14	2.271	1.36
	BO	3DFin	0.879	2.445	10.329	9.280	28.27	23.670	4.797	11.00	29.94	25.06	4.80	40	–2.96	5.25	2.064	1.39
		FSCT	0.924	1.789	7.560	9.280	28.27	23.670	5.205	12.05	29.36	24.55	5.20	40	–5.00	3.25	1.597	0.88
	SY	3DFin	0.571	2.136	7.199	22.520	35.54	29.673	1.634	27.00	32.91	30.41	1.63	52	–2.80	5.95	2.056	0.74
		FSCT	0.903	1.347	4.539	22.520	35.54	29.673	3.062	23.14	36.12	30.65	3.06	52	0.04	4.39	0.955	0.97
	MY	3DFin	0.931	2.216	12.812	7.760	26.52	17.295	4.596	10.75	26.89	18.97	4.60	142	–0.39	6.39	1.482	1.68
		FSCT	0.988	1.190	6.883	7.760	26.52	17.295	5.158	8.63	27.32	18.33	5.16	142	0.10	2.64	0.595	1.04
	MO	3DFin	0.771	1.853	8.086	12.580	28.37	22.920	2.882	14.27	28.30	23.41	2.88	34	–3.23	4.68	1.829	0.49
		FSCT	0.975	0.803	3.503	12.580	28.37	22.920	3.658	13.75	28.70	23.47	3.66	34	–0.65	1.47	0.596	0.55

Appendix A3. The error distribution Diameter at the Breast Height.

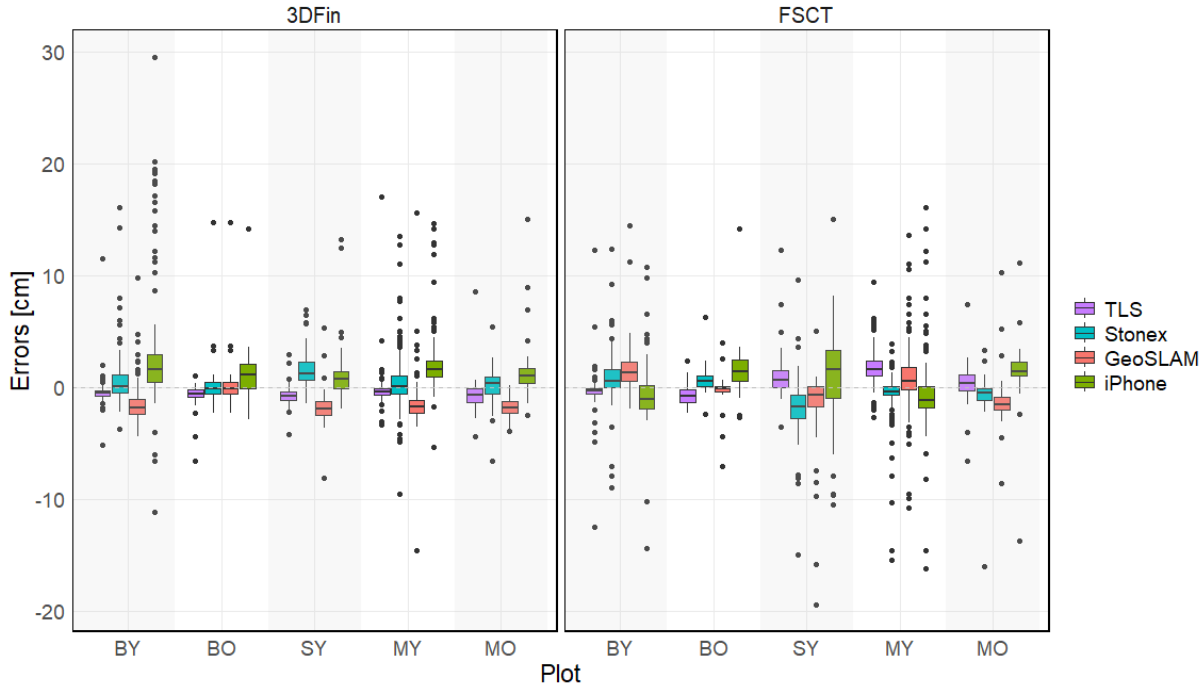

Appendix A4. The error distribution Tree Height

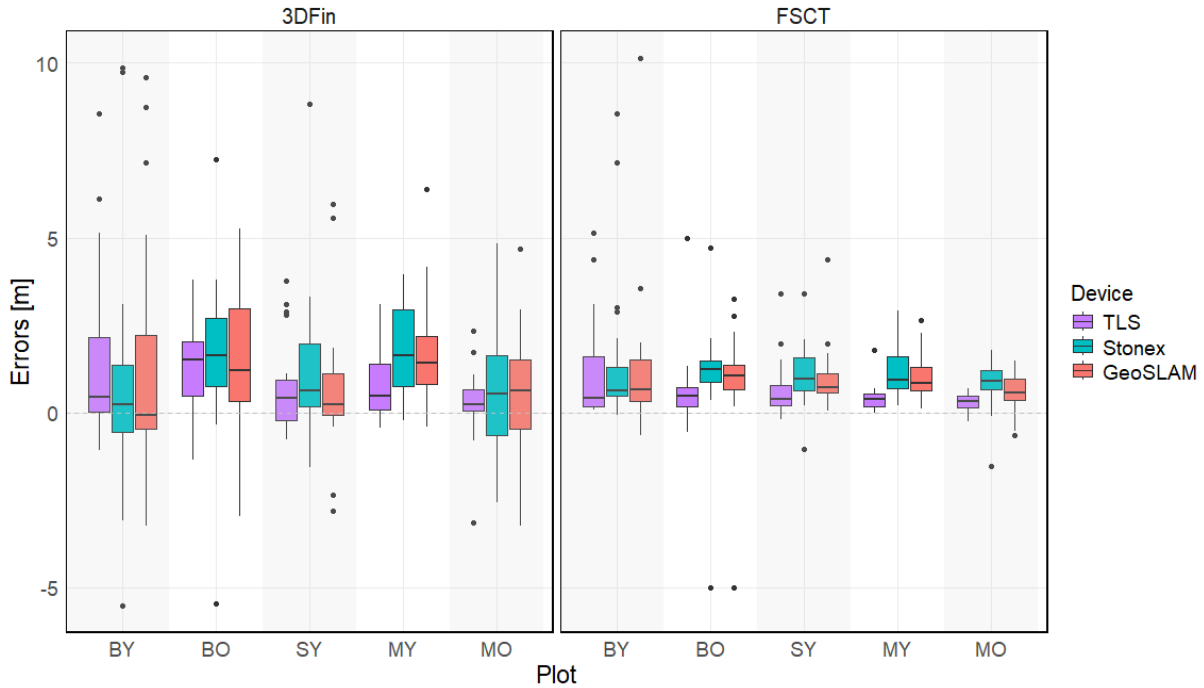

Appendix A5. Canopy point cloud comparison.

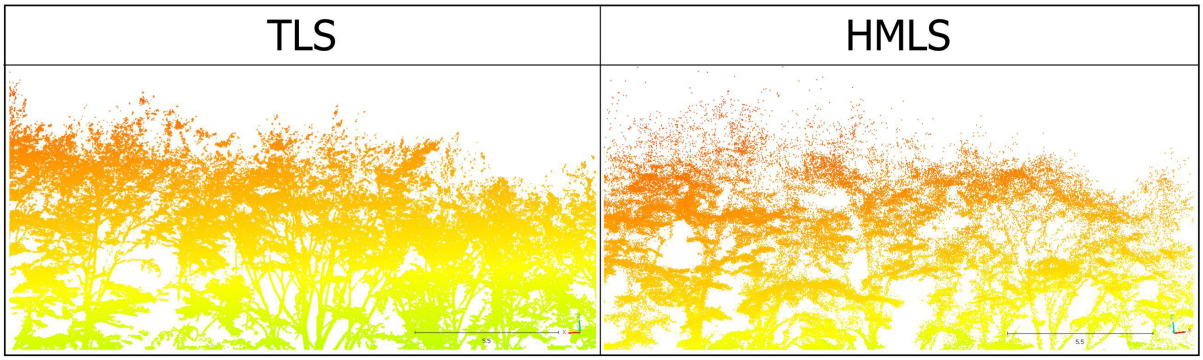

Appendix A6. The point clouds of young spruce, the red points show 5 cm slices at the height of 1.3 m from the ground (GeoSLAM ZEB Horizon based point cloud).

Appendix A7. Comprehensive comparison of 3DFin and FSCT in terms of accuracy and practical application. Values are normalized (0 = best, 1 = worst), so results closer to the center indicate better performance, while those near the edge indicate worse performance.

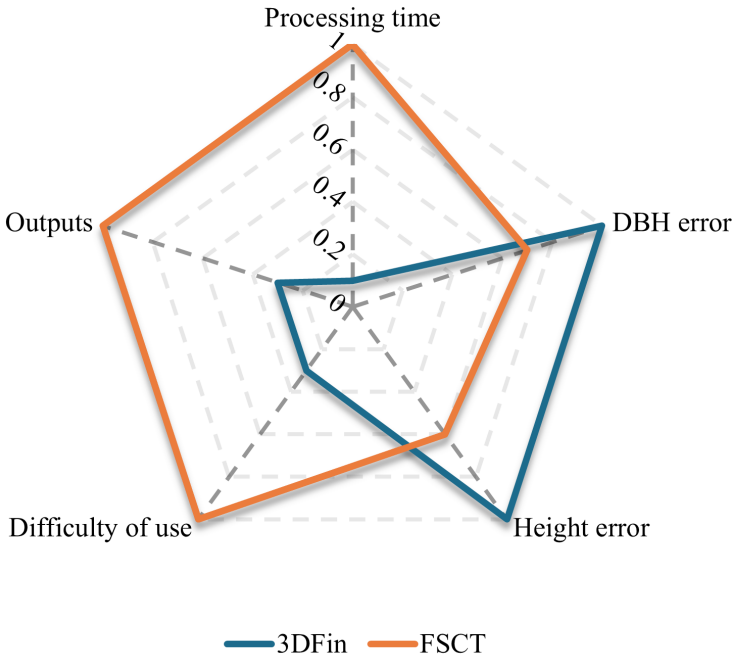

Appendix A8. Comprehensive comparison of ground-based LiDAR devices for monitoring of forest ecosystems in terms of accuracy and practical application. Values are normalized (0 = best, 1 = worst), so results closer to the center indicate better performance, while those near the edge indicate worse performance.